



Mangrove distribution and diversity during three Cenozoic thermal maxima in the Northern Hemisphere (pollen records from the Arctic–North Atlantic–Mediterranean regions)

Speranta-Maria Popescu¹  | Jean-Pierre Suc² | Séverine Fauquette³ |
Mostefa Bessedik⁴ | Gonzalo Jiménez-Moreno⁵ | Cécile Robin⁶ | Loïc Labrousse²

¹GeoBioStratData.Consulting, Rillieux-la-Pape, France

²Sorbonne Université, CNRS-INSU, Institut des Sciences de la Terre Paris, ISTeP UMR 7193, Paris, France

³ISEM, Univ. Montpellier, CNRS, IRD, EPHE, Montpellier, France

⁴Département des Sciences de la Terre, Laboratoire de Paléontologie Stratigraphique et Paléoenvironnement, Université d'Oran 2 Mohamed Ben Ahmed, Oran, Algeria

⁵Departamento de Estratigrafía y Paleontología, Universidad de Granada, Granada, Spain

⁶Université de Rennes, CNRS, Géosciences Rennes-UMR 6118, Rennes, France

Correspondence

Speranta-Maria Popescu, Geobiostratdata. Consulting, 385 route du Mas Rillier, 69140 Rillieux-la-Pape, France.
Email: speranta.popescu@gmail.com

Funding information

IODP-France; Total S.A.; Université de Rennes 1; Université Sorbonne Paris Cité; Agence Nationale de la Recherche

Handling Editor: Mark Bush

Abstract

Aim: Past pollen records reveal the changes in latitudinal distribution of plants in relation to climate, particularly their expansion in response to global warming. The maximum northward expansion of the mangrove genus *Avicennia* since the Early Eocene is known, but this information is missing for other mangrove taxa. Here, we evaluate the diversity of past mangroves with respect to latitude during three Cenozoic thermal maxima (PETM: 56 Ma; EECO: 54–49 Ma; MMCO: 17–14 Ma).

Location: North Atlantic, Mediterranean.

Taxa: *Avicennia*, other mangrove taxa (Rhizophoraceae, *Nypa*, *Xylocarpus*, *Pelliciera*, etc.).

Method: We collected well-dated marine sediments along a Northern Hemisphere latitudinal transect and we analysed their pollen content in order to compare the past distribution of mangrove taxa with the present. The analysis of 89 samples (PETM: 13; EECO: 31; MMCO: 45) was performed and interpreted using a robust botanical background for identification of pollen grains and their representativeness in marine sediments.

Results: During the Early Eocene, two palaeolatitudinal thresholds at 65–70°N and 35°N, respectively, delimited the *Avicennia*-only mangrove from a diversified but scrawny mangrove and finally from a diversified and well-developed mangrove. The *Avicennia* threshold was selective at 40°N during the Mid-Miocene. The *Avicennia* range limit was up to 10–15° poleward of the limit for other mangrove taxa during the Early Eocene and the Mid-Miocene compared with 9° at present.

Main conclusions: A buffer zone characterised by a diversified but scrawny mangrove co-occurring with a few megathermal plants occurred in the Early Eocene between 35°N and 65–70°N. This finding questions the relative influence of a more 'equable' climate and/or the ability of some taxa to expand towards areas with cooler conditions in the past. Mangrove provincialism, which was established progressively after the Early Eocene, was probably forced by plate tectonics. The taxonomic impoverishment of the Atlantic East Pacific province was probably caused by successive periods of global cooling. These results support the Tethyan origin of the mangroves.

KEYWORDS

Avicennia, climate change, Eocene–Miocene, mangrove, range limit, thermal optimum

1 | INTRODUCTION

Inter-tropical mangrove vegetation comprises major trees such as *Avicennia*, Rhizophoraceae (*Rhizophora*, *Bruguiera*, *Ceriops*, *Kandelia*), *Nypa*, *Sonneratia*, and other less abundant plants such as *Excoecaria*, *Xylocarpus*, *Pelliciera*, *Aegialitis*, *Heritiera*, *Scyphiphora* and *Brownlowia* (Tomlinson, 1986). Mangrove distribution today reveals latitudinal differences between different geographical areas partly due to the influence of marine currents and partly due to plant sensitivity to different air and water temperatures (Figure 1; Duke, 1992; Duke et al., 1998; Kao et al., 2004; Osland et al., 2017; Tomlinson, 1986). If >1,000 mm, annual rainfall is also an important factor affecting the distribution, stature and diversity of mangroves (Bardou et al., 2020; Osland et al., 2017). Mangrove establishment is closely linked to hydrodynamics and, particularly, to sea-level changes (Woodroffe et al., 2016).

Avicennia occurs in a slightly wider latitudinal range than *Rhizophora*, but the generally observed latitudinal difference between these genera (median value 1.8°) is 8–9° in northern New Zealand and southern Australia (Quisthoudt et al., 2012). Although the lowest temperature limits tolerated by *Avicennia* (e.g. 8.1°C minimum air temperature, 12.7°C minimum water temperature) differ significantly from those tolerated by *Rhizophora* (e.g. 13.1°C minimum air temperature, 16.4°C minimum water temperature), the difference is not enough to explain the observed differences in latitude distribution (Quisthoudt et al., 2012). Freezing appears to be a critical factor in limiting mangrove expansion (Stuart et al., 2007) while resistance to freezing

may drive the northward expansion of North American mangrove in response to current climate warming (Bardou et al., 2020; Cook-Patton et al., 2015).

Avicennia and *Rhizophora* are emblematic mangrove genera because they occur in both the Atlantic East Pacific (AEP) and Indo-West Pacific (IWP) provinces although they are represented by different species (Figure 1; Duke et al., 1998; Ellison et al., 1999; Tomlinson, 1986). Some genera only occur in one of the provinces (*Pelliciera* to the west; *Sonneratia*, *Xylocarpus* and *Nypa* to the east; Figure 1).

The discovery of mangrove vegetation consisting of only *Avicennia* inhabiting the Mediterranean shorelines during the Miocene (Bessedik, 1981a) advanced our knowledge of mangrove history (Plaziat et al., 2001; Srivastava & Prasad, 2019). More recently and surprisingly, *Avicennia* was recorded up to Arctic latitudes and even near the North Pole during the Early Eocene (Salpin et al., 2019; Suan et al., 2017; Suc et al., 2020). Accordingly, the following question arose: did the poleward limit of *Avicennia* compared with that of the other mangrove taxa increase or decrease after the Early Eocene? To answer this question, pollen records containing mangrove taxa from three Cenozoic thermal maxima were selected for comparison with present-day mangrove distribution: Palaeocene–Eocene Thermal Maximum (PETM: 56 Ma; Westerhold et al., 2015), Early Eocene Climatic Optimum (EECO: 54–49 Ma; Westerhold et al., 2020) and Mid-Miocene Climatic Optimum (MMCO: 17–14 Ma; Zachos et al., 2001). The Early Eocene pollen records in which *Avicennia* is the only mangrove tree are limited to the Arctic domain (Salpin et al., 2019; Suan et al., 2017; Suc et al., 2020), and the Mid-Miocene pollen

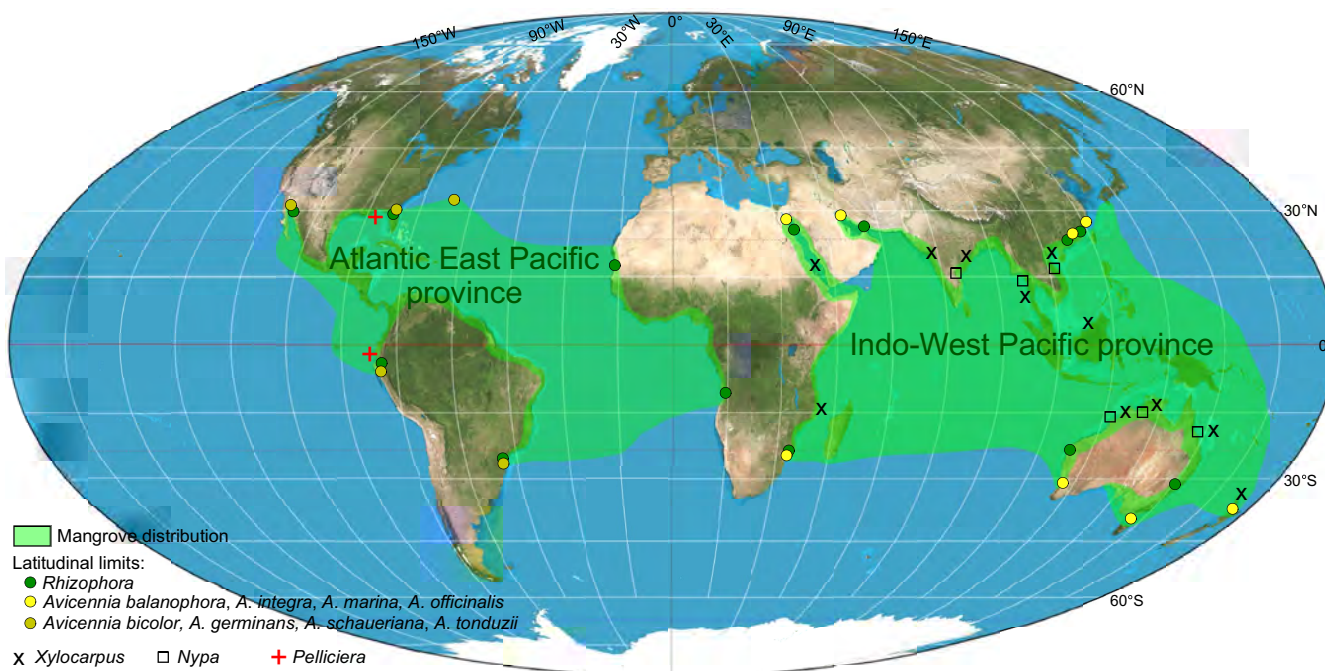


FIGURE 1 Present-day geographic distribution of mangroves with respect to their two provinces with information on occurrence of some taxa according to Tomlinson (1986) and latitudinal limits of *Avicennia* and *Rhizophora* according to Quisthoudt et al. (2012). The used geographic map is from Strebe, D. R. - CC BY-SA 3.0 (Mollweide projection equal-area), <https://commons.wikimedia.org/w/index.php?curid=16115320>



records in which *Avicennia* is the only mangrove tree are limited to the Mediterranean domain (Bessedik, 1981a, 1981b, 1984; Jiménez-Moreno et al., 2008; Jiménez-Moreno & Suc, 2007). Hence, we chose to focus on the North Atlantic by analysing new locations and using earlier data (Table S1). The results of this work may inform potential future distribution and diversity of mangroves in response to current climate warming with the need to provide increasing protection against anthropic damage (Giri et al., 2011).

2 | MATERIALS AND METHODS

The pollen records concerned are shown on the palaeogeographical maps in Figure 2 (PETM and EECO) and Figure 3 (MMCO) and listed in Table S1. They were aligned along an Atlantic latitudinal transect (including the Mediterranean region for the MMCO) to enable us to locate the threshold which separates the diversified mangrove

from impoverished mangrove containing only *Avicennia*. The study concerns clayey sediments which are usually excellent deposits for pollen preservation.

The pollen data from each location have been dated independently, most often by micropalaeontology, as specified in Table S1. We selected the pollen spectra that indicated the warmest conditions in the selected records where the expected warming event is diffuse. The duration of each pollen record was appraised by fitting the pollen assemblages and their variations to the reference oxygen isotope curve within the originally defined biostratigraphical interval (see Figure S1 and explanation herein).

Palaeolatitude estimates were deduced from the global Eulerian rotation poles database from Torsvik et al. (2012), using the Palaeolatitude.org online toolbox (van Hinsbergen et al., 2015) and then compared to regional maps. Uncertainties vary from ± 2 to ± 3 latitude degrees. For location 1 in the PETM (Figure 2), uncertainty might be higher due to the uncertain position of the Lomonosov Ridge

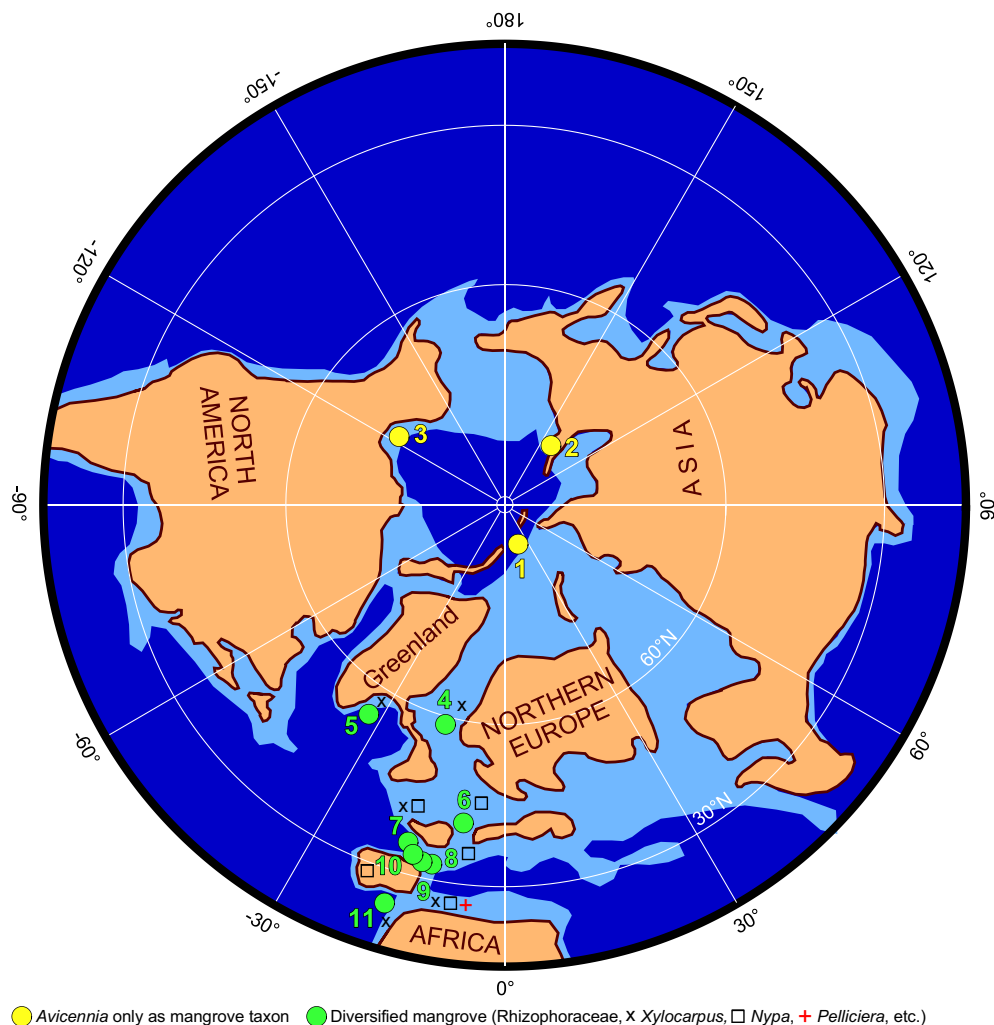


FIGURE 2 Palaeocene–Eocene (PETM) and early Eocene (EECO) mangrove pollen records (with information on the occurrence of some taxa) along a North–South transect. Palaeogeographical map with estimated palaeolatitudes (Polar orthographic Projection) is from Backman et al. (2006) and Eberle and Greenwood (2012), modified by Suc et al. (2020). Locations: 1, Site M0004A; 2, Faddeevsky Island; 3, Caribou Hills; 4, Site 343; 5, Site 918; 6, Kallio 027E148; 7, Noirmoutier; 8, Calavanté 1; 9, Morlaàs 1; 10, Gan; 11, Site 547

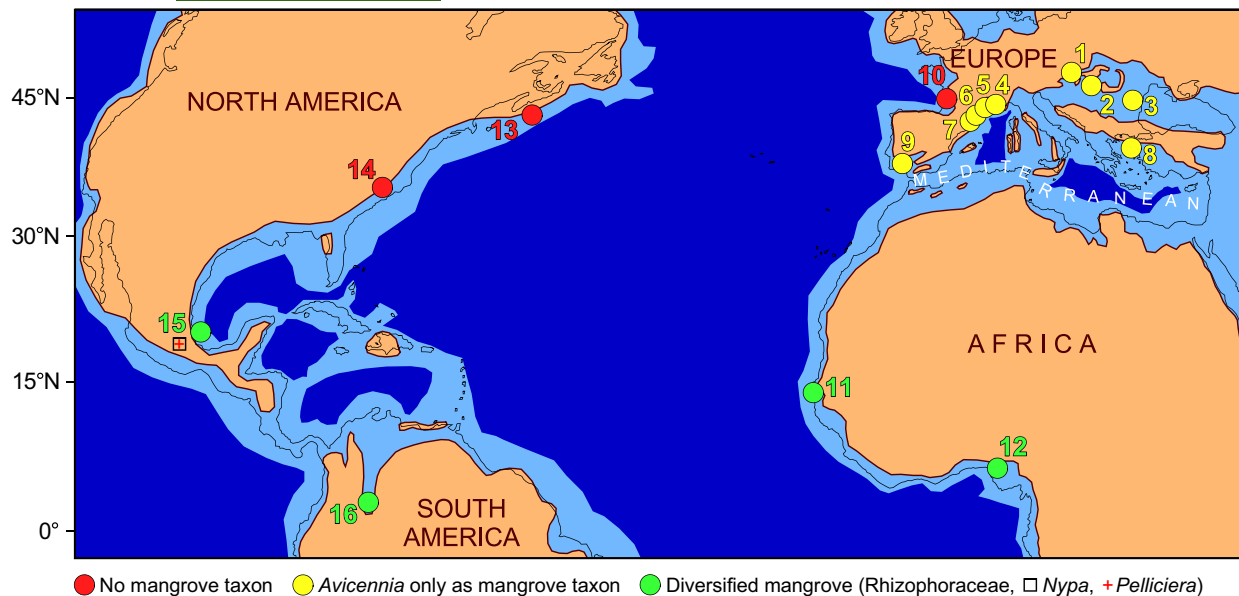


FIGURE 3 Mid-Miocene (MMCO) mangrove pollen records (with information on the occurrence of some taxa) along a North-South transect. Palaeogeography is from Rögl (1999) and Jolivet et al. (2006) for the Mediterranean region *s.l.* Atlantic-Pacific palaeogeography is from Herold et al. (2009), Scotese (2014), and Cao et al. (2017). The current geographic outline is from Strebe, D. R. – CC BY-SA 3.0 (Mollweide projection equal-area), <https://commons.wikimedia.org/w/index.php?curid=16115320>. The estimated palaeolatitude of each location is indicated in Table S1.

Locations: 1, Göllersdorf; 2, Herend 46; 3, Balgarevo C136A; 4, Les Mées 1, Châteauredon; 5, Estagel, Bayanne; 6, Narbonne V. Hugo College, Lespignan II, Montady, Saint-Géniès, Montagnac, Mèze, Loupian, Issanka, Poussan, Montbazin; 7, La Rierussa, Sant Pau d'Ordal; 8 Kultak; 9, Alboran A1; 10, Laborde 1D; 11, Bignona well; 12, Niger Delta well M1; 13, Site M00027; 14, Alum Bluff; 15, La Herradura; 16, Apaporis River.

prior to the Eurasian Basin opening but conservative reconstructions place it north of Greenland since 70 Ma (Gion et al., 2017). The 76°N and 78°N palaeolatitudes are probably minimum estimates for PETM and EECO at location 1, respectively (Table S1). The computed position of location 3 (Figure 2) during the EECO is consistent with recent regional palaeogeographical reconstructions (Table S1; Eberle & Greenwood, 2012). For European sites and the Tethyan realm, computed palaeolatitudes are systematically 6° to 7° lower than those mentioned in regional reconstructions (Meulenkamp & Sissingh, 2003). This discrepancy is mainly explained by the northward rotation of extra-Alpine stable Europe since 50 Ma at least (Torsvik et al., 2008). For the MMCO, as locations 2, 8 and 9 are situated in unconstrained mobile regions, their palaeolatitude was deduced from latitude changes at adjacent locations.

The samples analysed in this work, plus those analysed earlier by our team (Table S1), were processed using a standard protocol: acid digestion (HCl, HF), concentration using $ZnCl_2$ (at density 2.0), and sieving through a 10- μm nylon mesh. A 40 μl volume of residue was mounted between the coverslip and microscope slide using glycerol.

The major methodological and conceptual contribution of this study is the use of a botanical approach for the Palaeogene samples. This approach was made possible by considering all the morphological characters of the pollen instead of just a few (often secondary). Details on *Avicennia* and other mangrove taxa are provided in Supporting Information (Figures S1–S10). In addition, we performed pollen counts (at least 100–150 pollen grains per sample excluding over-represented taxa such as *Pinus*), which is another novelty.

Pollen data are shown in synthetic pollen diagrams (Figures 4–6) where the taxa are grouped according to both their present-day ecological significance and to their behaviour during the Cenozoic (Table S2; Suc et al., 2018, 2020).

Taxa are mainly grouped according to the thermal classification of Nix (1982) with some emphasis on the woody mangrove: *Avicennia*; other mangrove taxa; other megathermal plants which require a mean annual temperature (MAT) higher than 24°C; megamesothermal plants that require a MAT between 24 and 20°C; mesothermal plants that require a MAT between 20 and 14°C; *Pinus* plus indeterminate Pinaceae devoid of thermal significance because of their low level in botanical identification; meso-microthermal plants that require a MAT between 14 and 12°C; microthermal plants that require a MAT under 12°C; plants of no significance because of their cosmopolitan status at the family or genus level; Cupressaceae *p.p.* (*Cupressus-Juniperus* type); herbaceous plants. A complete list of the identified taxa and additional details on the ecological groups of plants are provided in Table S2.

Some reconstructed terrestrial palaeoclimate parameters taken from pollen records are used to discuss our results. These data come from the Climatic Amplitude Method (Fauquette et al., 1998), which, based on comparison with >6000 present-day pollen records distributed worldwide, relies on the relationship between the relative abundance of each taxon and the climate. To obtain more refined estimates, this method accounts not only for the occurrence/absence criterion but also for pollen grain percentages. The reconstructed climatic values concern the low-elevation vegetation,

meso-microthermal and microthermal taxa being excluded from the process. *Pinus*, which inhabits different vegetation belts, from the lowest to the highest belts, especially in the Mediterranean region, was also excluded from the calculation.

The advantage of applying this 'Quaternary-Neogene' palynological approach to the Palaeogene samples is that it not only provides reliable information on the palaeo-ecosystems but also helps to establish robust homogeneous data.

Marine pollen records are reliable indicators of the occurrence of mangrove vegetation along the shoreline whether they are supplied by air or fluvial transport as demonstrated by studies on modern pollen sedimentation (Bengo, 1996; Caratini et al., 1987; Hooghiemstra et al., 1986; Phuphumirat et al., 2016; Poumot, 1989; Somboon, 1990). For some of the study areas, the distance travelled by mangrove pollen grains is more than a few kilometres, indeed even after several dozen kilometres percentages can be 5%-10% of the pollen sum (Bengo, 1996; Caratini et al., 1987; Hooghiemstra et al., 1986). Such data are of great importance for the reliability of our past mangrove records, all located relatively close to the land (Figures 2-3). In addition, some modern pollen records show high variability in mangrove pollen percentages with respect to the whole pollen flora: the highest

percentages are recorded in front of large mangroves, the lowest percentages in front of weakened mangroves (Bengo, 1996; Caratini et al., 1987; Hooghiemstra et al., 1986) or dwarf mangroves (Willard et al., 2001). It will be recalled that in these modern records, *Avicennia* pollen is usually under-represented in comparison with other mangrove taxa, particularly Rhizophoraceae (e.g. Somboon, 1990).

3 | RESULTS

3.1 | Palaeocene-Eocene Thermal Maximum

Avicennia was the only mangrove taxon we recorded in the Arctic pollen floras (locations 1-2; Figures 2 and 4). These floras were also very poor in megathermal plants, as they are only represented

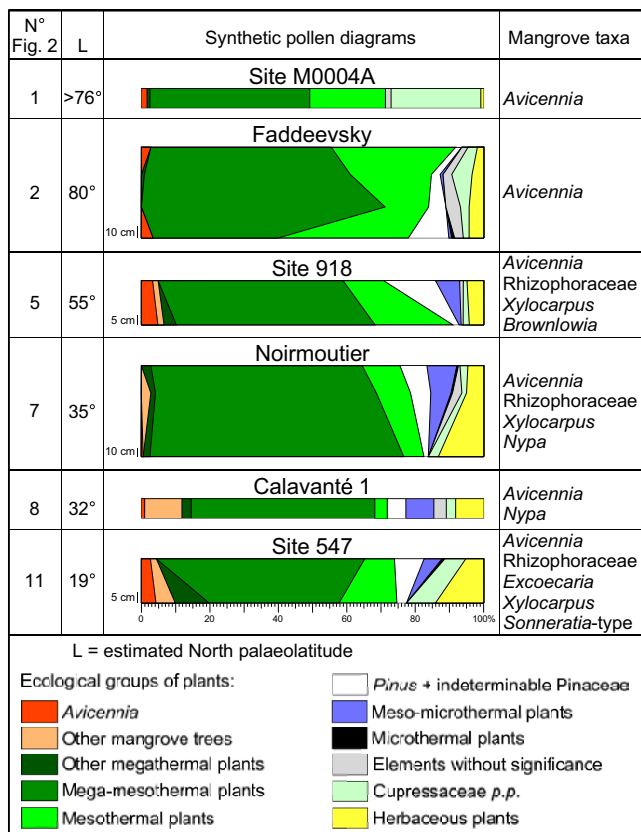


FIGURE 4 Synthetic diagrams of PETM pollen records arranged according to their estimated palaeolatitude with listing of their mangrove woody taxa. Site Number (No) refers to Figure 2. Detail of taxa constituting the ecological groups of plants is given in Table S2. For locations made of several samples, the thickness scale is indicated to the left of the diagram

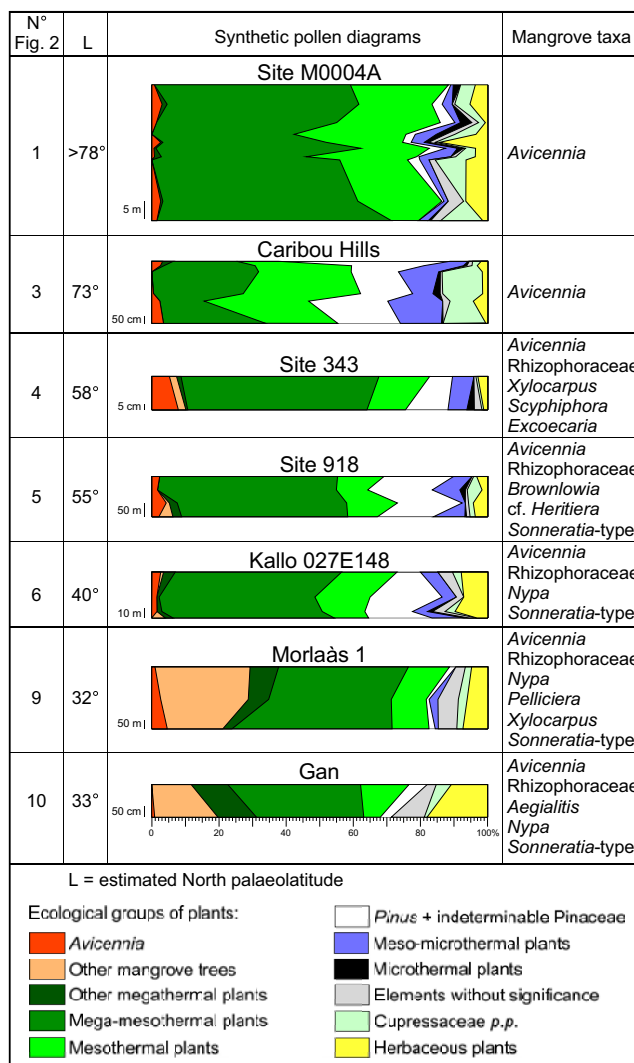


FIGURE 5 Synthetic diagrams of EECO pollen records arranged according to their estimated palaeolatitude with listing of their mangrove woody taxa. Site Number (No) refers to Figure 2. For locations made of several samples, the thickness scale is indicated to the left of the diagram

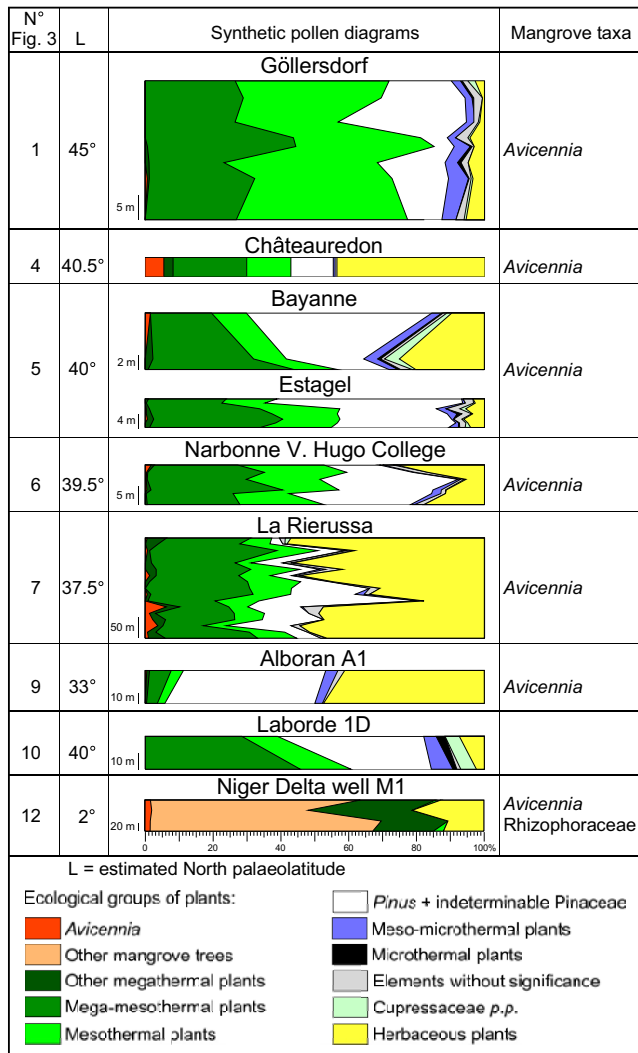


FIGURE 6 Synthetic diagrams of some selected MMCO pollen records arranged according to their estimated palaeolatitude with listing of their mangrove woody taxa. Site Number (No) refers to Figure 3. For locations made of several samples, the thickness scale is indicated to the left of the diagram

by two taxa, both at very low percentages (Figure 4; Table S2). In southern Greenland (location 5; Figure 2), larger quantities of *Avicennia* were recorded than in Arctic samples, along with a small number of other mangrove taxa (Rhizophoraceae, *Xylocarpus* and *Brownlowia*) and small percentage of a few megathermal plants (Figure 4; Table S2). At Noirmoutier (location 7; Figure 2), *Avicennia* was rarely recorded but small percentages documented three other mangrove trees (Rhizophoraceae, *Xylocarpus* and *Nypa*) and megathermal plants (Figure 4; Table S2). In the North Pyrenean Gulf (location 8; Figure 2), *Avicennia* pollen was found in small quantities with high percentages of *Nypa* and moderate amounts of a few megathermal plants (Figure 4; Table S2). Offshore northwestern Africa (location 11; Figure 2), *Avicennia* was found abundantly along with several other mangrove trees (Rhizophoraceae, *Excoecaria*, *Xylocarpus* and possibly *Sonneratia*-type—see comment in Supporting Information) in equal quantities

and with significant percentages of some megathermal plants (Figure 4; Table S2).

3.2 | Early Eocene Climatic Optimum

As in the PETM, *Avicennia* was the only mangrove tree recorded in the Arctic pollen floras during the EECO (locations 1 and 3; Figures 2 and 5). These floras were also very poor in megathermal plants which were only represented by very small percentages of six taxa (Figure 5; Table S2). We found *Avicennia* pollen in significantly larger quantities with low percentages of other mangrove taxa (Rhizophoraceae, *Xylocarpus*, *Brownlowia*, *Scyphiphora*, *Excoecaria*, cf. *Heritiera* and possibly *Sonneratia*-type) offshore northwestern Europe and offshore southern Greenland (locations 4 and 5; Figures 2 and 5). A similar pollen flora characterised the Belgium Basin (location 6; Figure 2) where *Avicennia* was accompanied by Rhizophoraceae, *Nypa* and *Sonneratia*-type and an increasing number of megathermal plants (Figure 5; Table S2). Small to moderate quantities of *Avicennia* pollen were observed in the North Pyrenean Gulf (locations 9–10; Figure 2), along with a large quantity of *Nypa* and several other woody mangrove taxa (Rhizophoraceae, *Pelliciera*, *Xylocarpus*, *Aegialitis* and *Sonneratia*-type); the accompanying megathermal plants were abundant and present at significant percentages (Figure 5; Table S2).

3.3 | Mid-Miocene Climatic Optimum

The northernmost known pollen flora consisting of only *Avicennia* indicating mangrove vegetation, occurred together with very few megathermal taxa, was located at 45°N palaeolatitude (location 1; Figures 3 and 6). *Avicennia* was commonly recorded south of 41°N (locations 4–7), usually at a low percentage except at locations 4 and 7, and with no other mangrove taxa (Figures 3 and 6; Tables S1 and S2). Megathermal plants were diversified at locations 4 and 7 but at relatively low percentages (Figures 3 and 6; Table S2). In contrast, location 10 (Figure 3) contained neither *Avicennia* pollen nor megathermal plants, despite being at an almost similar palaeolatitude to locations 4–6 on the Atlantic side (Figure 6; Table S2).

4 | DISCUSSION

Three thermal optima were chosen as periods during which climatic conditions favoured maximum spreading of *Avicennia*, and possibly other mangrove taxa accompanied by diverse megathermal taxa, towards high latitudes. In addition, the distribution and diversity of past mangroves during particularly warm periods can be compared to the present-day context characterised by climate warming. The results we obtained from our analyses of pollen floras located along a latitudinal transect in the Northern Hemisphere in both the Atlantic and Mediterranean regions provide new insights into several aspects including (1) the occurrence



of latitudinal thresholds leading to successive steps in mangrove development, (2) the spread of the latitudinal limit of *Avicennia* in relation to other mangrove taxa, (3) the onset of the present mangrove provinces and (4) location of mangrove refuges during colder periods. But before interpreting our results, we review the representativeness of the occurrence/absence of mangrove pollen grains and the significance of their variations in abundance.

4.1 | Representativeness of mangrove pollen and implications of its quantitative variations

The three past warm intervals studied correspond to episodes with high global sea level characterised by major elevations (up to 80 m in the PETM and 60 m in the EECO and MMCO; Miller et al., 2020). During the longer climatic optima such as EECO and MMCO, the global sea level fluctuated somewhat (50 m in the EECO, 40 m in the MMCO) under the direct forcing of global temperature variations (Miller et al., 2020). Variations in mangrove pollen in our long pollen records in the EECO (Site M0004A, Caribou Hills, Kallu O27E148) and MMCO (Göllersdorf, Narbonne V. Hugo College, La Rierussa) may, according to their correlation with the oxygen isotope curve (Figure S1), have been caused by these secondary changes in sea level, which, in any case, resulted from global temperature changes. The same interpretation could be applied to the other locations of shorter duration.

The available reconstructed palaeoclimatic conditions indicate that the annual rainfall was higher than 1,000 mm at many locations:

- In the PETM: Faddeevsky (Suan et al., 2017), Site M0004A (Suc et al., 2020), Calavanté 1 (Fauquette, in progress);
- In the EECO: Caribou Hills (Salpin et al., 2019), Site M0004A (Suc et al., 2020), Morlaàs 1 and Gan (Fauquette, in progress);
- In the MMCO: Göllersdorf (Jiménez-Moreno et al., 2008), Estagel (Fauquette et al., 2007), Narbonne V. Hugo College (Fauquette, in progress).

Only the MMCO records from La Rierussa and Alboran A1 indicate annual precipitation slightly lower and significantly lower than 1,000 mm, respectively (Fauquette et al., 2007). This low precipitation does not seem to have affected the abundance of *Avicennia* pollen in La Rierussa. This can be compared to the modern distribution of *Avicennia* in the sub-desertic Red Sea region. Conversely, it could be the cause of the small quantity of *Avicennia* pollen in the Alboran A1 well. Accordingly, annual precipitation does not seem to have played a critical role in the distribution and development of mangroves during the three climatic optima considered here, except at the southernmost location in the Mediterranean in the MMCO.

The reconstructed mean temperature of the coldest month is evidence for the absence of freezing episodes during the PETM and EECO in the Arctic domain (Salpin et al., 2019; Suan et al., 2017; Suc et al., 2020). In this region, the first appearance of

ephemeral continental ice seems more recent than 38 Ma (see: Suc et al., 2020). Similarly, the reconstructed mean temperature of the coldest month for the northernmost *Avicennia* locations during the MMCO suggests a lack of freezing episodes (Fauquette, unpublished data).

We conclude that, at the macroecological (geographical and chronological) scales of our study, sea and land temperatures were the main factors that controlled the development and diversity of the mangrove forests during the Palaeogene and Neogene climatic optima.

4.2 | Latitudinal thresholds in the Northern Hemisphere separated diversified mangroves from *Avicennia*-only mangroves

4.2.1 | PETM and EECO

The abundance of pollen records in the EECO allowed us to reconstruct an almost continuous latitudinal gradient of mangrove distribution in the North Atlantic region (Figures 2 and 5; Table S1). A first palaeolatitudinal threshold was identified, at about 58–73°N, delimiting the transition from a mangrove ecosystem with only *Avicennia* (locations 1, 3) to a diversified mangrove ecosystem. A second palaeolatitudinal threshold was identified at about 32–40°N which separated pollen records where the abundance of the other mangrove taxa was less than 5% with little diversity of megathermal plants (locations 4–6) from pollen records where the abundance of the other mangrove taxa was higher than 5% with a relatively high diversity of megathermal flora (locations 9–10; Figure 5). The value of 5% of other mangrove taxa allowed us to define a scrawny though diversified mangrove between 32°N and 40°N and a well-developed diversified mangrove below 32°N. The same palaeolatitude thresholds were inferred for the PETM, at about 55–76°N and 32–35°N, respectively (Figure 4). The large amount of *Avicennia* pollen recorded at location 5 may be explained by the existence of a protected area offshore southern Greenland (Figure 2).

Mangrove expansion depends on air temperatures but chiefly on sea temperatures. Today, *Avicennia* species are generally limited to coastal areas characterised by a warm climate with sea surface temperatures (SSTs) around 22.6°C (Quisthoudt et al., 2012) and cannot tolerate extremely cold air temperatures (below –4°C; Cavanaugh et al., 2014). However, thanks to warm marine currents, *Avicennia* is the only mangrove plant that is not limited to the tropics and can occur at SSTs as low as 15.6°C at its coldest limit in New Zealand and eastern Australia (Quisthoudt et al., 2012). *Rhizophora* requires slightly higher SSTs, even at its coldest limit (SSTs >20.8°C; Quisthoudt et al., 2012). Model simulations of the sea surface (SSTs) and terrestrial MATs realised for the PETM and EECO along Earth's latitudinal range give too low temperature estimates and do not provide any evidence for a significantly reduced equator-to-pole temperature gradient (e.g. Hollis et al., 2012; Huber & Caballero, 2011; Lunt et al., 2012; Zhu et al., 2020).

The only one consistent with the palaeoclimate estimated through tetraether lipids (Weijers et al., 2007) and pollen records (Suan et al., 2017; Suc et al., 2020), although SSTs and MATs estimated north of 70° are also too low, reveals a sharp drop in the SST curve between palaeolatitude 65°N and 70°N (Figure 7; Sagoo et al., 2013) that could limit the distribution of the more thermophilous mangrove taxa such as Rhizophoraceae as evidenced in our pollen data (Table 1). Moreover, the inversion of MATs and SSTs curves at ~37°N (Sagoo et al., 2013) corresponds in our data to the transition from diversified but scrawny mangrove to diversified and well-developed mangrove at about 35°N (Figure 7; Table 1). These inflexions in the marine and atmospheric temperature curves may record Early Eocene mangrove distribution and diversification in the Northern Hemisphere. Evidence for a similar threshold is shown in the Southern Hemisphere at palaeolatitude 65°S characterised by the occurrence of an Early Eocene scrawny mangrove with only *Nypa* in Tasmania (Table 1; Pole and Macphail, 1996). These thresholds should be taken into account to review the so-called Early Eocene 'equable' climate (Sloan & Barron, 1990).

Two challenging-correlating interpretations can be proposed:

1. Are the coupled climate models affected by insufficient performance under greenhouse conditions? It is now generally accepted (e.g. Sagoo et al., 2013);
2. Are temperature estimates from proxies exaggerated? Do tetraether lipids over-estimate temperatures or are the temperature requirements attributed to *Avicennia* in estimations based on pollen, too warm? This is possible, but the results based on kaolinite content of sediments in New Siberia (Suan et al., 2017), by MAT estimated in Antarctica (Pross et al., 2012) and TEX86-derived

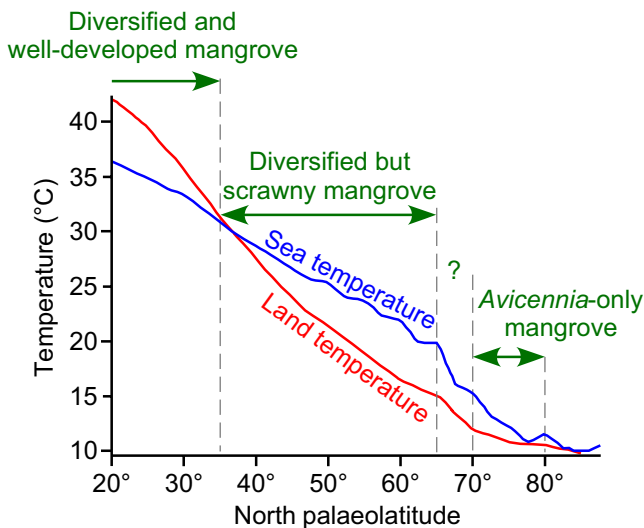


FIGURE 7 Sea surface temperature (SST) vs. land (air) mean annual temperature (MAT) and mangrove distribution and diversification in the North Hemisphere during the Early Eocene (simulation E17 from: Sagoo et al., 2013)

TABLE 1 Latitudinal distribution and diversification of mangroves during three noteworthy thermal maxima compared to Present

PETM and EECO		MMCO		Present		Hemisphere
Palaeolatitude	Mangrove type	Palaeolatitude	Mangrove type	Latitude	Mangrove type	
70–80°N	<i>Avicennia</i> -only mangrove					N
60–70°N	No data					O
35–60°N	Diversified but scrawny mangrove					R
<35°N	Diversified and well-developed mangrove	33–45°N	<i>Avicennia</i> -only mangrove	30–31.8°N	<i>Avicennia</i> -only mangrove	T
		15–33°N	No data	<30°N	Diversified and well-developed mangrove	H
		?<20°N	Diversified and well-developed mangrove			
65°S	<i>Nypa</i>	<30°S	Diversified and well-developed mangrove	<30°S	Diversified and well-developed mangrove	S
		30–39°S	<i>Avicennia</i> -only mangrove	30–39°S	<i>Avicennia</i> -only mangrove	O
						U
						T
						H



SSTs in Tasmania (Bijl et al., 2009) are in line with pollen-based estimates. To answer these questions, we need to understand the process and magnitude of Arctic temperature amplification, especially seasonality, which is observed in the present global warming (Riboldi et al., 2020) and is believed to have been intense during the PETM and EECO (Frieling et al., 2017; Huber & Caballero, 2011; Lunt et al., 2012).

The inherent forcing of solar radiation should be examined as an outcome. Indeed, studying the Mid-Holocene latitudinal variation of insolation controlling the temperature gradient, Davis and Brewer (2009) provide evidence for a threshold at 47°N delimiting increased summer insolation at higher latitudes but reduced insolation at lower latitudes and a threshold between 60 and 70°N of the June insolation. Loutre et al. (2004) reconstruct global insolation for the Late Quaternary and provide evidence for a phase reversal at 43–44°N with prevalence of obliquity forcing over climate at higher latitudes and eccentricity at lower latitudes, the difference in mean annual irradiance being particularly marked above 70°N. An Early Eocene latitudinal reconstruction of insolation with the respective effect of winter vs. summer irradiance could allow to check if such thresholds forced the progressive diversity of mangrove ecosystems and the distribution of its major components.

4.2.2 | MMCO

A threshold at about 40°N seems to have existed during the MMCO in the Mediterranean region, separating the *Avicennia* mangrove based on the abundance of *Avicennia* pollen and/or megathermal plants (Figure 6). The difference is particularly well expressed at locations 4 and 7 compared to location 1. Location 4 (Châteauredon) probably benefited from protected environmental conditions at the far end of a narrow gulf.

Our data concern the northern shorelines of the Mediterranean region where no other mangrove taxon was recorded. The lack of coeval pollen data from the southern Mediterranean shorelines does not allow us to hypothesise their occurrence a few latitudinal degrees southward. In this direction (Figure 3), the first available pollen data are those from La Herradura (location 15: Palacios Chavez & Rzedowski, 1993) and from the coastal area of Senegal (location 11: Médus, 1975). Unfortunately, these pollen floras are not really usable because of their chronological imprecision and unavailable pollen data. However, their abundant pollen illustrations support the occurrence of *Nypa* and *Pelliciera* at La Herradura and that of *Rhizophora* at both locations. In addition, observation of the pollen photographs published convinces us of the occurrence of *Avicennia* at the two locations (detailed in Supporting Information). Close to the palaeo-equator, location 12 (well M1 from the Niger Delta; Durugbo & Olayiwola, 2017) shows evidence of abundant *Rhizophora* and scarce *Avicennia* pollen grains during a stratigraphical interval attributable to the Mid-Miocene, the redrawing of which is provided in Figure 6 for comparison with the Mediterranean pollen floras. At location 16 (Lower Apaporis River;

Figure 3), Hoorn (2006) documents the occurrence of *Rhizophora* and *Mauritia* (Arecaceae). This comparison suggests that the diversity of the AEP mangrove was already significantly impoverished in the Mid-Miocene.

The MMCO has been modelled and sea surface and/or terrestrial temperature simulations are available (e.g. Goldner et al., 2014; Herold et al., 2011; You et al., 2009). Herold et al. (2011) reconstructed terrestrial MATs that are characterised by strong dip variations between 30 and 35°N with a temperature gradient of 1.5°C per degree in latitude, which is significantly higher than the modern temperature gradient (0.6°C per degree in latitude) and very much higher than the temperature gradient obtained for the MMCO from pollen records in Western Europe (0.48°C per degree in latitude: Fauquette et al., 2007). In addition, the proposed terrestrial MATs for the latitudinal interval 30–42°N are significantly lower (11–17°C) than those estimated from pollen data in the Mediterranean domain (18.2–20.5°C, Fauquette et al., 2007; Jiménez-Moreno et al., 2008). Accordingly, there is a marked discrepancy in the MATs for the MMCO between the model simulation and pollen proxy, as in the SSTs between the model simulation and biomarker proxy (Salocchi et al., 2021), similarly to previous time periods. As hypothesised above, it is possible that too much weight was attributed to *Avicennia* and/or the few megathermal plants in the temperature reconstructions based on pollen records. However, it is well known that for the MMCO, like for the previous periods, climate models generally fail to reproduce the polar amplification and lead to over-estimation of the equator to pole temperature gradient (e.g. Goldner et al., 2014; You et al., 2009). It is also possible that, like today, the Mediterranean Basin was a particular climatic region that allowed *Avicennia* to survive in slightly lower thermal conditions and to develop in some propitious contexts (locations 4 and 7; Figure 6; Table S1). This assumption is supported by some evidence: (1) the unexpected very rare presence of *Avicennia* pollen in the southernmost pollen flora (location 9: Figures 3 and 6); (2) the absence of *Avicennia* and of any megathermal taxon at location 10 on the Atlantic shoreline at a northwestern Mediterranean palaeolatitude (Figures 3 and 6; Table S1); and the absence of *Avicennia* and of any megathermal taxon at the West Atlantic locations 13 and 14 corresponding to southernmost Mediterranean palaeolatitudes.

4.3 | Northernmost latitudinal limit of *Avicennia* distribution with respect to the diversified mangrove

Today, the northernmost distribution of *Avicennia* is limited to a latitude range of 1.8° of the diversified mangrove (Figure 1; Table 1; Quisthoudt et al., 2012). In the Middle Miocene (MMCO), this interval may have reached latitude range of about 15°, an interval that could be exaggerated considering the lack of data between palaeolatitudes 33°N (location 9) and 15°N (location 15; Figures 3 and 6–7; Table 1). During the Early Eocene (PETM and EECO), this geographical difference in latitude would have been about 10–15° (Figures 2, 4–5 and 7; Table 1). Obviously, the size of the gap is linked with



warmth, even if the temperature may have been somewhat higher in the Mediterranean Basin, which was probably sheltered from cold air masses. Today, there is a latitudinal difference of about 9° in *Avicennia* distribution between mangrove consisting only of *Avicennia* and diversified mangrove in the South Hemisphere, illustrating the high potential thermal flexibility of the genus (Figure 1; Table 1; Quisthoudt et al., 2012).

To summarise, the maximum latitudinal gap for *Avicennia* distribution outside diversified mangrove could have been 15° during the three Cenozoic thermal maxima, which matches the 9° observed today and accounts for uncertainty in palaeolatitude estimates.

The simultaneous occurrence of several (PETM) and many (EECO) megathermal plants including mangrove taxa (represented by abundant pollen grains; Figures 4–5; Table S2) marks diversified and well-developed mangrove. Considering the maximum latitudinal expansion of this mangrove, there is no or little latitudinal difference between the Early Eocene and today, which would be feasible in the case of an 'equable' climate during the Early Eocene (Figure 7; Table 1). However, a buffer zone between 35 and 65–70°N, where we recorded a diversified but scrawny mangrove with only few megathermal companions for the Early Eocene (Figures 4–5 and 7; Table 1; Table S2), questions the relative influence of a more 'equable' climate and the ability of some taxa to invade cooler areas in the past. During the Middle Miocene, disregarding the probable peculiar environmental context of the Mediterranean domain (Figure 3), the moderate diversity in megathermal plants expressed by low pollen percentages (Figure 6; Table S2) suggests a transition between the buffer zone and the *Avicennia* mangrove, as witnessed during the Early Eocene, and signals the gradual withdrawal of the mangrove in Europe.

4.4 | What is the relationship between the past *Avicennia*-only and diversified mangroves and the present mangrove provinces?

Avicennia comprises eight modern species (The Plant List, 2013) equally distributed in the AEP province (*A. bicolor*, *A. germinans*, *A. schaueriana* and *A. tonduzii*) and IWP province (*A. balanophora*, *A. integra*, *A. marina* and *A. officinalis*; Dahdouh-Guebas, 2020). Some morphological characters make it possible to distinguish these species by their pollen (Thanikaimoni, 1987), as supported by our own observations (Figures S1–S3).

Precise observation of Early Eocene *Avicennia* pollen grains from the Arctic indicates the occurrence of several species, some specimens being very close to the modern species *A. germinans*, *A. marina* and *A. officinalis* (Figures S1 and S2; Salpin et al., 2019; Suan et al., 2017; Suc et al., 2020). The same variety in *Avicennia* pollen morphology is observed in the other pollen records from the Early Eocene Atlantic latitudinal transect (Figure 2: locations 4–11: Figures S6–S9), suggesting similar specific diversity to that considered at the higher palaeolatitudes. According to the present geographical distribution of the three above-mentioned

Avicennia species, it appears that no mangrove provincialism existed during the Early Eocene, in agreement with evidence at locations 4–11 (Figures 2 and 4–5; Tables S1 and S2), in addition to the Rhizophoraceae, of *Nypa* and *Xylocarpus*, currently restricted to the IWP province (Figure 1; Tomlinson, 1986). *Pelliciera*, now confined to the AEP province (Figure 1; Tomlinson, 1986), was already present in the Atlantic domain (location 9: Figures 2 and 5; Tables S1 and S2). These data are robust and support a Tethyan origin of mangroves, consequently, the regional taxonomic diversity resulted from the continental drift and not from an Indo-Pacific centre of origin (Ellison et al., 1999; Morley, 1999; Plaziat et al., 2001; Srivastava & Prasad, 2019).

A cluster of probably two *Avicennia* species inhabited the Mediterranean domain during the Middle Miocene with pollen indicating *A. marina* and *A. officinalis* (Figures S3 and S10; Bessedik, 1981b). Today, these species belong to the IWP province, thereby contributing to the persistence of *Avicennia* in western Europe, favoured by large marine connections to the east while, at the same time, the eastern Atlantic shoreline is devoid of this taxon at similar palaeolatitudes (Figure 3). This could argue for provincial differentiation almost completely achieved during the Miocene, if not the ultimate occurrence of *Nypa* along the western Atlantic shoreline (location 15: Figure 3; Palacios Chavez & Rzedowski, 1993). The more restricted distribution of *Pelliciera* in the AEP province is confirmed by pollen flora found at location 15 (Figure 3; Palacios Chavez & Rzedowski, 1993).

These data lead us to conclude that mangrove provincialism progressively established itself after the Early Eocene warm period, probably forced by plate tectonics, the taxonomic impoverishment of the AEP province probably being caused by successive global colder periods (Plaziat et al., 2001; Srivastava & Prasad, 2019).

4.5 | Persistence of mangrove during cooler periods between thermal optima

Our study focuses only on the three warmest episodes of the last 60 Ma but mangrove history obviously continued in the meantime. Here, we only recall or complete some items of this history, which was already summarised by Ellison et al. (1999), Plaziat et al. (2001) and Srivastava and Prasad (2019).

Considering its high expansion up to the northernmost latitudes during the PETM and EECO, logically *Avicennia* rarely occurred in the Arctic region up to the Mid-Eocene Climatic Optimum (MECO: 40 Ma; Suc et al., 2020). This late occurrence in the Arctic region also questions the potential ability of *Avicennia* to persist during cooler periods and/or its possible latitudinal shifts between the EECO and MECO, unless the thermal amplitude suggested by the $\delta^{18}\text{O}$ curves is over-estimated. Its southward retreat is illustrated by one last Early Oligocene occurrence (with no other mangrove taxon) at Site 345 (NW Norway; study in progress). Only *Avicennia* was present in the northwestern Mediterranean Oligocene (study in progress), where it persisted up to the earliest Serravallian (Bessedik, 1984; Jiménez-Moreno & Suc, 2007). The youngest record of *Avicennia* at similar



palaeolatitude on the European side of the Atlantic belongs to the early Burdigalian. *Avicennia* persisted in the southern Mediterranean and Atlantic Morocco up to the late Messinian (Suc et al., 2018). The ultimate reliable record of *Avicennia* concerns the Early Pliocene in the southern Black Sea (Biltekin et al., 2015). *Avicennia* expansions and retreats very closely mirror increases and decreases in temperature, respectively, and were driven by the opportune opening or persistence of marine gateways.

The most recent evidence of a diversified and well-developed mangrove in the northwestern Mediterranean Basin was in the Bartonian (c. 40 Ma) with, in addition to *Avicennia*, *Pelliciera*, *Bronlowia*, *Nypa*, *Heritiera* and *Aegiceras* (Cavagnetto & Anadón, 1995). A scrawny mangrove was still present during the Oligocene in northern Turkey, including *Avicennia*, *Pelliciera* and *Nypa* (Akgün et al., 2013). These data complete the information on the process of disjunction of the modern mangrove biogeographical provinces, which occurred during the Late Eocene and Oligocene and ended in the earliest Neogene.

5 | CONCLUSION

A set of 11 pollen floras arranged along a North Atlantic latitudinal transect were analysed using a botanical approach and provide information on mangrove distribution and diversity during the warmest Palaeogene phases (PETM and EECO). Evidence is provided for two palaeolatitudinal thresholds, at, respectively, 65–70°N and 35°N, separating the *Avicennia*-only mangrove (which reached 80°N) from a diversified but scrawny mangrove, and then from a diversified and well-developed mangrove. These thresholds, which moderate the so-called Early Eocene 'equable' climate hypothesis, were probably due to latitudinal changes in temperature and possibly in solar irradiation. The latitudinal gap between the northward expansion of *Avicennia* and diversified mangrove during the three Cenozoic thermal maxima (10–15°) could have been almost similar to the southward gap observed today in Australia (9°; Table 1). This mangrove organisation once more reveals significant discrepancies between models and proxies, unless the temperature estimates deduced from *Avicennia* and some mangrove and other megathermal plants have been somewhat exaggerated when these taxa only are represented by a few pollen grains. A similar expansion event occurred during the MMCO but chiefly concerned *Avicennia*, which benefited from propitious conditions in the Mediterranean Basin documented by nine pollen records, also suggesting *Avicennia*'s possibly greater adaptive ability in the past.

Our results concerning the Early Eocene North Atlantic and Arctic mangroves provide the missing link to robustly support the Tethyan origin of mangroves, the provincialism of which started in the Late Eocene probably forced by continental drift, and ended in the Early Neogene. The subsequent global colder periods probably played a key role impoverishing the Western mangroves.

ACKNOWLEDGEMENTS

We are grateful to the IODP Bremen Core Repository for the continuous consideration of our requests for samples. Paul Bernier, Peter Stassen, Noël Vandenberghe and Nadia Barhoun provided samples. This work benefited from very fruitful discussions with Jean-Claude Plaziat. The PYRAMID project (ANR, France) provided significant financial support for Eocene investigations in the Northern Pyrenees (sampling field trips, obtaining sediment core samples, sample analyses). The successive studies of the Early Eocene in the Arctic domain benefited from grants by Sorbonne University, Rennes 1 University, Total S.A. and IODP-France. O. Boudouma is acknowledged for technical assistance with scanning electronic microscopy. Two anonymous referees and the editor, Mark Bush, are particularly acknowledged for their constructive comments and their overall assessment of our manuscript. No permits are needed to carry out the work. Publication ISEM No 2021-165 SUD.

CONFLICT OF INTEREST

The authors declare that they have no conflict of interest.

DATA AVAILABILITY STATEMENT

The detailed pollen data are stored in the Dryad repository URL for the Miocene pollen records: <https://doi.org/10.5061/dryad.n02v6wxxn>; URL for the Eocene pollen records: <https://doi.org/10.5061/dryad.4j0zpc8bt>.

ORCID

Speranta-Maria Popescu  <https://orcid.org/0000-0001-5345-395X>

REFERENCES

- Akgün, F., Akkiraz, M. S., Üçbaş, S. D., Bozcu, M., Kapan Yeşilyurt, S., & Bozcu, A. (2013). Oligocene vegetation and climate characteristics in north-west Turkey: Data from the south-western part of the Thrace Basin. *Turkish Journal of Earth Sciences*, 22, 277–303. <https://doi.org/10.3906/yer-1201-3>
- Backman, J., Moran, K., McInroy, D. B., Mayer, L. A., & the Expedition 302 Scientists. (2006). Sites M0001–M0004. *Proceedings of the Integrated Ocean Drilling Program*, 302, 1–169. <https://doi.org/10.2204/iodp.proc.302.104.2006>
- Bardou, R., Parker, J. D., Feller, I. C., & Cavanaugh, K. C. (2020). Variability in the fundamental versus realized niches of North American mangroves. *Journal of Biogeography*, 48, 160–175. <https://doi.org/10.1111/jbi.13990>
- Bengo, M. D. (1996). *La sédimentation pollinique dans le Sud-Cameroun et sur la plateforme marine à l'époque actuelle et au Quaternaire récent: étude des paléoenvironnements* (PhD thesis). University of Montpellier.
- Bessedik, M. (1981a). Une mangrove à *Avicennia* L. en Méditerranée occidentale au Miocène inférieur et moyen. Implications paléogéographiques. *Comptes-Rendus de l'Académie des Sciences de Paris*, ser. 2, 293, 469–472.
- Bessedik, M. (1981b). *Recherches palynologiques sur quelques sites du Burdigalien du midi de la France* (PhD thesis). University of Montpellier.

- Bessedik, M. (1984). The early Aquitanian and upper Langhian–lower Serravallian environments in the Northwestern Mediterranean region. *Paléobiologie Continentale*, 14(2), 153–179.
- Bijl, P. K., Schouten, S., Sluijs, A., Reichert, G.-J., Zachos, J. C., & Brinkhuis, H. (2009). Early Palaeogene temperature evolution of the south-west Pacific Ocean. *Nature*, 461, 776–779. <https://doi.org/10.1038/nature08399>
- Biltekin, D., Popescu, S.-M., Suc, J.-P., Quézel, P., Jiménez-Moreno, G., Yavuz, N., & Çağatay, M. N. (2015). Anatolia: A long-time plant refuge area documented by pollen records over the last 23 million years. *Review of Palaeobotany and Palynology*, 215, 1–22. <https://doi.org/10.1016/j.revpalbo.2014.12.004>
- Cao, W., Zahirovic, S., Flament, N., Williams, S., Golonka, J., & Müller, R. D. (2017). Improving global paleogeography since the Paleozoic using paleobiology. *Biogeosciences*, 14, 5425–5439. <https://doi.org/10.5194/bg-14-5425-2017>
- Caratini, C., Tastet, J.-P., Tissot, C., & Frédoux, A. (1987). Sédimentation palynologique actuelle sur le plateau continental de Côte d'Ivoire. *Mémoires et Travaux de l'École Pratique des Hautes Etudes, Institut de Montpellier*, 17, 69–100.
- Cavagnetto, C., & Anadón, P. (1995). Une mangrove complexe dans le Bartonien du bassin de l'Ebre (NE de l'Espagne). *Palaeontographica*, B, 236, 147–165.
- Cavanaugh, K. C., Kellner, J. R., Forde, A. J., Gruner, D. S., Parker, J. D., Rodriguez, W., & Feller, I. C. (2014). Poleward expansion of mangroves is a threshold response to decreased frequency of extreme cold events. *Proceedings of the National Academy of Sciences of the United States of America*, 111, 723–727. <https://doi.org/10.1073/pnas.1315800111>
- Cook-Patton, S. C., Lehmann, M., & Parker, J. D. (2015). Convergence of three mangrove species towards freeze-tolerant phenotypes at an expanding range edge. *Functional Ecology*, 29, 1332–1340. <https://doi.org/10.1111/1365-2435.12443>
- Dahdouh-Guebas, F. (2020). *World mangroves database*. Retrieved from <http://www.vliz.be/vmcdcd/mangroves>
- Davis, B. A. S., & Brewer, S. (2009). Orbital forcing and role of the latitudinal insolation/temperature gradient. *Climate Dynamics*, 32, 143–165. <https://doi.org/10.1007/s00382-008-0480-9>
- Duke, N. C. (1992). Mangrove floristics and biogeography. *Coastal and Estuarine Studies*, 41, 63–101.
- Duke, N. C., Ball, M. C., & Ellison, J. C. (1998). Factors influencing biodiversity and distributional gradients in mangroves. *Global Ecology and Biogeography Letters*, 7, 27–47. <https://doi.org/10.2307/2997695>
- Durugbo, E. U., & Olayiwola, M. A. (2017). Palynological dating and palaeoenvironments of the M1 well, Middle Miocene, Niger Delta, Nigeria. *Palaeontologia Africana*, 52, 46–57.
- Eberle, J. J., & Greenwood, D. R. (2012). Life at the top of the greenhouse Eocene world—A review of the Eocene flora and vertebrate fauna from Canada's High Arctic. *Geological Society of America Bulletin*, 124, 3–23. <https://doi.org/10.1130/B30571.1>
- Ellison, A. M., Farnsworth, E. J., & Merkt, R. E. (1999). Origin of mangrove ecosystems and the mangrove biodiversity anomaly. *Global Ecology and Biogeography*, 8, 95–115.
- Fauquette, S., Guiot, J., & Suc, J.-P. (1998). A method for climatic reconstruction of the Mediterranean Pliocene using pollen data. *Palaeogeography, Palaeoclimatology, Palaeoecology*, 144, 183–201. [https://doi.org/10.1016/S0031-0182\(98\)00083-2](https://doi.org/10.1016/S0031-0182(98)00083-2)
- Fauquette, S., Suc, J.-P., Jiménez-Moreno, G., Micheels, A., Jost, A., Favre, E., Bachiri Taoufiq, N., Bertini, A., Clet-Pellerin, M., Diniz, F., Farjanel, G., Feddi, N., & Zheng, Z. (2007). Latitudinal climatic gradients in Western European and Mediterranean regions from the Mid-Miocene (c. 15 Ma) to the Mid-Pliocene (c. 3.5 Ma) as quantified from pollen data. In M. Williams, A. Haywood, J. Gregory, & D. N. Schmidt (Eds.), *Deep-time perspectives on climate change. Marrying the signal from computer models and biological proxies* (pp. 481–502). The Micropaleontological Society, The Geological Society, Special Publications.
- Frieling, J., Gebhardt, H., Huber, M., Adekeye, O. A., Akande, S. O., Reichard, G.-J., Middelburg, J. J., Schouten, S., & Sluijs, A. (2017). Extreme warmth and heat-stressed plankton in the tropics during the Paleocene-Eocene Thermal Maximum. *Science Advances*, 3, e1600891. <https://doi.org/10.1126/sciadv.1600891>
- Gion, A. M., Williams, S. E., & Müller, E. D. (2017). A reconstruction of the Eureka Orogeny incorporating deformation constraints. *Tectonics*, 36, 304–320. <https://doi.org/10.1002/2015TC004094>
- Giri, C., Ochieng, E., Tieszen, L. L., Zhu, Z., Singh, A., Loveland, T., Masek, J., & Duke, N. (2011). Status and distribution of mangrove forests of the world using earth observation satellite data. *Global Ecology and Biogeography*, 20, 154–159. <https://doi.org/10.1111/j.1466-8238.2010.00584.x>
- Goldner, A., Herold, N., & Huber, M. (2014). The challenge of simulating the warmth of the mid-Miocene climatic optimum in CESM. *Climate of the Past*, 10, 523–536. <https://doi.org/10.5194/cp-10-523-2014>
- Herold, N., Huber, M., & Müller, R. D. (2011). Modeling the Miocene climate optimum. Part I: Land and atmosphere. *Journal of Climate*, 24, 6353–6372. <https://doi.org/10.1175/2011JCLI4035.1>
- Herold, N., You, Y., Müller, R. D., & Seton, M. (2009). Climate model sensitivity to changes in Miocene paleotopography. *Australian Journal of Earth Sciences*, 56, 1049–1059. <https://doi.org/10.1080/0812090903246170>
- Hollis, C. J., Taylor, K. W. R., Handley, L., Pancost, R. D., Huber, M., Creech, J. B., Hines, B. R., Crouch, E. M., Morgans, H. E. G., Crampton, J. S., Gibbs, S., Pearson, P. N., & Zachos, J. C. (2012). Early Paleogene temperature history of the Southwest Pacific Ocean: Reconciling proxies and models. *Earth and Planetary Science Letters*, 349–350, 53–66. <https://doi.org/10.1016/j.epsl.2012.06.024>
- Hooghiemstra, H., Agwu, C. O. C., & Beug, H.-J. (1986). Pollen and spore distribution in recent marine sediments: A record of NW-African seasonal wind patterns and vegetation belts. *"Meteor" Forschungs-Ergebnisse*, ser. C, 40, 87–135.
- Hoorn, C. (2006). Mangrove forests and marine incursions in Neogene Amazonia (Lower Apaporis River, Colombia). *Palaaios*, 21(2), 206–219. <https://doi.org/10.2110/palo.2005.p05-131>
- Huber, M., & Caballero, R. (2011). The early Eocene equable climate problem revisited. *Climate of the Past*, 7, 603–633. <https://doi.org/10.5194/cp-7-603-2011>
- Jiménez-Moreno, G., Fauquette, S., & Suc, J.-P. (2008). Vegetation, climate and palaeoaltitude reconstructions of the Eastern Alps during the Miocene based on pollen records from Austria, Central Europe. *Journal of Biogeography*, 35, 1638–1649. <https://doi.org/10.1111/j.1365-2699.2008.01911.x>
- Jiménez-Moreno, G., & Suc, J.-P. (2007). Middle Miocene latitudinal climatic gradient in Western Europe: Evidence from pollen records. *Palaeogeography, Palaeoclimatology, Palaeoecology*, 253, 224–241. <https://doi.org/10.1016/j.palaeo.2007.03.040>
- Jolivet, L., Augier, R., Robin, C., Suc, J.-P., & Rouchy, J. M. (2006). Lithospheric-scale geodynamic context of the Messinian salinity crisis. *Sedimentary Geology*, 188–189, 9–33. <https://doi.org/10.1016/j.sedgeo.2006.02.004>
- Kao, W.-Y., Shih, C.-N., & Tsai, T.-T. (2004). Sensibility to chilling temperatures and distribution differ in the mangrove species *Kandelia candel* and *Avicennia marina*. *Tree Physiology*, 24, 859–864.
- Loutre, M.-F., Paillard, D., Vimeux, F., & Cortijo, E. (2004). Does mean annual insolation have the potential to change the climate? *Earth and Planetary Science Letters*, 221, 1–14. [https://doi.org/10.1016/S0012-821X\(04\)00108-6](https://doi.org/10.1016/S0012-821X(04)00108-6)
- Lunt, D. J., Dunkley Jones, T., Heinemann, M., Huber, M., LeGrande, A., Winguth, A., Loptson, C., Marotzke, J., Roberts, C. D., Tindall, J., Valdes, P., & Winguth, C. (2012). A model–data comparison for a multi-model ensemble of early Eocene atmosphere–ocean simulations: EoMIP. *Climate of the Past*, 8, 1717–1736. <https://doi.org/10.5194/cp-8-1717-2012>



- Médus, J. (1975). Palynologie de sédiments tertiaires du Sénégal méridional. *Pollen et Spores*, 17(4), 545–608.
- Meulenkamp, J. E., & Sissingh, W. (2003). Tertiary palaeogeography and tectonostratigraphic evolution of the Northern and Southern Peri-Tethys platforms and the intermediate domains of the African-Eurasian convergent plate boundary zone. *Palaeogeography, Palaeoclimatology, Palaeoecology*, 196, 209–228. [https://doi.org/10.1016/S0031-0182\(03\)00319-5](https://doi.org/10.1016/S0031-0182(03)00319-5)
- Miller, K. G., Browning, J. V., Schmelz, W. J., Kopp, R. E., Mountain, G. S., & Wright, J. D. (2020). Cenozoic sea-level and cryospheric evolution from deep-sea geochemical record and continental margin records. *Science Advances*, 6, eaaz1346.
- Morley, R. J. (1999). *Origin and evolution of tropical rain forests*. J. Wiley & Sons Ltd.
- Nix, H. (1982). Environmental determinants of biogeography and evolution in Terra Australis. In W. R. Barker & P. J. M. Greenslade (Eds.), *Evolution of the flora and fauna of arid Australia* (pp. 47–66). Peacock Publishing.
- Osland, M. J., Feher, L. C., Griffith, K. T., Cavanaugh, K. C., Enwright, N. M., Day, R. H., Day, R. H., Stagg, C. L., Krauss, K. W., Howard, R. J., Grace, J. B., & Rogers, K. (2017). Climatic controls on the global distribution, abundance, and species richness of mangrove forests. *Ecological Monographs*, 87(2), 341–359. <https://doi.org/10.5066/F78C9TDM>
- Palacios Chavez, R., & Rzedowski, J. (1993). Estudio palinológico de las floras fosiles del Miocene inferior y principios del Miocene medio de la region de Pichucalco, Chiapas, Mexico. *Acta Botánica Mexicana*, 24, 1–96.
- Phumphumirat, W., Zetter, R., Hofmann, C.-C., & Ferguson, D. K. (2016). Pollen distribution and deposition in mangrove sediments of the Ranong Biosphere Reserve, Thailand. *Review of Palaeobotany and Palynology*, 233, 22–43. <https://doi.org/10.1016/j.revpalbo.2016.06.007>
- Plaziat, J.-C., Cavagnetto, C., Koeniguer, J.-C., & Baltzer, F. (2001). History and biogeography of the mangrove ecosystem, based on a critical reassessment of the paleontological record. *Wetlands Ecology and Management*, 9, 161–179.
- Pole, M. S., & Macphail, M. K. (1996). Eocene *Nypa* from Regatta Point, Tasmania. *Review of Palaeobotany and Palynology*, 92, 55–67. [https://doi.org/10.1016/0034-6667\(95\)00099-2](https://doi.org/10.1016/0034-6667(95)00099-2)
- Poumot, C. (1989). Palynological evidence for eustatic events in the tropical Neogene. *Bulletin des Centres de Recherche Exploration-Production Elf-Aquitaine*, 13(2), 437–453.
- Pross, J., Contreras, L., Bijl, P. K., Greenwood, D. R., Bohaty, S. M., Schouten, S., Bendle, J. A., Röhl, U., Tauxe, L., Raine, J. I., Huck, C. E., van de Flierdt, T., Jamieson, S. S. R., Stickle, C. E., van de Schootbrugge, B., Escutia, C., Brinkhuis, H., & Integrated Ocean Drilling Program Expedition 318 Scientists. (2012). Persistent near-tropical warmth on the Antarctic continent during the early Eocene epoch. *Nature*, 488, 73–77. <https://doi.org/10.1038/nature11300>
- Quisthoudt, K., Schmitz, N., Randin, C. F., Dahdouh-Guebas, F., Robert, E. M. R., & Koedam, N. (2012). Temperature variation among mangrove latitudinal range limits worldwide. *Trees*, 26, 1919–1931. <https://doi.org/10.1007/s00468-012-0760-1>
- Riboldi, J., Lott, F., D'Andrea, F., & Rivièrè, G. (2020). On the linkage between Rossby Wave phase speed, atmospheric blocking, and Arctic Amplification. *Geophysical Research Letters*, 47, e2020GL087796. <https://doi.org/10.1029/2020GL087796>
- Rögl, F. (1999). Mediterranean and Paratethys. Facts and hypotheses of an Oligocene to Miocene paleogeography (short overview). *Geologica Carpathica*, 50, 339–349.
- Sagoo, N., Valdes, P., Flecker, R., & Gregoire, L. J. (2013). The Early Eocene equable climate problem: Can perturbations of climate model parameters identify possible solutions? *Philosophical Transactions of the Royal Society A: Mathematical, Physical and Engineering Sciences*, 371, 20130123. <https://doi.org/10.1098/rsta.2013.0123>
- Salocchi, A. C., Krawielicki, J., Eglinton, T. I., Fioroni, C., Fontana, D., Conti, S., & Picotti, V. (2021). Biomarker constraints on Mediterranean climate and ecosystem transitions during the Early-Middle Miocene. *Palaeogeography, Palaeoclimatology, Palaeoecology*, 562, 110092. <https://doi.org/10.1016/j.palaeo.2020.110092>
- Salpin, M., Schnyder, J., Baudin, F., Suan, G., Suc, J.-P., Popescu, M.-S., Fauquette, S., Reinhardt, L., Warmitz, M., & Labrousse, L. (2019). Evidence for subtropical warmth in Canadian Arctic (Beaufort-Mackenzie, Northwest Territories, Canada) during the early Eocene. In K. Piepjohn, J. V. Strauss, L. Reinhardt, & W. C. McClelland (Eds.), *Circum-Arctic structural events: Tectonic evolution of the Arctic margins and trans-Arctic links with adjacent orogens* (27, pp. 637–664), Geological Society of America Special Paper 541. [https://doi.org/10.1130/2018.2541\(27\)](https://doi.org/10.1130/2018.2541(27))
- Scotese, C. R. (2014). *Atlas of Neogene paleogeographic maps (Mollweide Projection)*. The Cenozoic, PALEOMAP Atlas for ArcGIS, PALEOMAP Project.
- Sloan, L. C., & Barron, E. J. (1990). “Equable” climates during Earth history? *Geology*, 18, 489–492.
- Somboon, J. R. P. (1990). Palynological study of mangrove and marine sediments of the Gulf of Thailand. *Journal of Southeast Asian Earth Sciences*, 4(2), 85–97. [https://doi.org/10.1016/0743-9547\(90\)90008-2](https://doi.org/10.1016/0743-9547(90)90008-2)
- Srivastava, J., & Prasad, V. (2019). Evolution and paleobiogeography of mangroves. *Marine Ecology*, 40, e12571. <https://doi.org/10.1111/maec.12571>
- Stuart, S. A., Choat, B., Martin, K. C., Holbrook, N. M., & Ball, M. C. (2007). The role of freezing in setting the latitudinal limits of mangrove forests. *New Phytologist*, 173, 576–583. <https://doi.org/10.1111/j.1469-8137.2006.01938.x>
- Suan, G., Popescu, S.-M., Suc, J.-P., Schnyder, J., Fauquette, S., Baudin, F., Yoon, D., Piepjohn, K., Sobolev, N. N., & Labrousse, L. (2017). Subtropical climate conditions and mangrove growth in Arctic Siberia during the early Eocene. *Geology*, 45, 539–542. <https://doi.org/10.1130/G38547.1>
- Suc, J.-P., Fauquette, S., Popescu, S.-M., & Robin, C. (2020). Subtropical mangrove and evergreen forest reveal Paleogene terrestrial climate and physiography at the North Pole. *Palaeogeography, Palaeoclimatology, Palaeoecology*, 551, 109755. <https://doi.org/10.1016/j.palaeo.2020.109755>
- Suc, J.-P., Popescu, S.-M., Fauquette, S., Bessedik, M., Jiménez Moreno, G., Bachiri Taoufiq, N., Zheng, Z., Médail, F., & Klotz, S. (2018). Reconstruction of Mediterranean flora, vegetation and climate for the last 23 million years based on an extensive pollen dataset. *Ecologia Mediterranea*, 44(2), 53–85. <https://doi.org/10.3406/ecmed.2018.2044>
- Thanikaimoni, G. (1987). Mangrove palynology. *Institut Français de Pondichéry, Travaux de la Section Scientifique et Technique*, 24, 1–100.
- The Plant List. (2013). Version 1.1. Published on the Internet. <http://www.theplantlist.org/>
- Tomlinson, P. B. (1986). *The botany of mangroves*. Cambridge University Press.
- Torsvik, T. H., Müller, R. D., Van der Voo, R., Steinberg, B., & Gaina, C. (2008). Global plate motion frames: toward a unified model. *Reviews of Geophysics*, 46, RG3004. <https://doi.org/10.1029/2007RG000227>
- Torsvik, T. H., Van der Voo, R., Preeden, U., Mac Niocaill, C., Steinberger, B., Doubrovine, P. V., van Hinsbergen, D. J. J., Domeier, M., Gaina, C., Tohver, E., Meert, J. G., McCausland, P. J. A., & Cocks, L. R. M. (2012). Phanerozoic polar wander, palaeogeography and dynamics. *Earth-Science Reviews*, 114, 325–368. <https://doi.org/10.1016/j.earscirev.2012.06.007>
- van Hinsbergen, D. J. J., de Groot, L. V., van Schaik, S. J., Spakman, W., Bijl, P. K., Sluijs, A., Langereis, C. G., & Brinkhuis, H. (2015). A paleolatitude calculator for paleoclimate studies. *PLoS One*, 10(6), e0126946. <https://doi.org/10.1371/journal.pone.0126946>
- Weijers, J. W. H., Schouten, S., Sluijs, A., Brinkhuis, H., & Sinninghe Damsté, J. S. (2007). Warm arctic continents during the Palaeocene-Eocene thermal maximum. *Earth Planetary and Science Letters*, 261, 230–238. <https://doi.org/10.1016/j.epsl.2007.06.033>

- Westerhold, T., Marwan, N., Drury, A. J., Liebrand, D., Agnini, C., Anagnostou, E., Barnet, J. S. K., Bohaty, S. M., De Vleeschouwer, D., Florindo, F., Frederichs, T., Hodell, D. A., Holbourn, A. E., Kroon, D., Lauretano, V., Littler, K., Lourens, L. J., Lyle, M., Pälike, H., ... Zachos, J. C. (2020). An astronomically dated record of Earth's climate and its predictability over the last 66 million years. *Science*, 369, 1383–1387. <https://doi.org/10.1126/science.aba6853>
- Westerhold, T., Röhl, U., Frederichs, T., Bohaty, S. M., & Zachos, J. C. (2015). Astronomical calibration of the geological timescale: Middle Eocene gap. *Climate of the Past*, 11, 1181–1195. <https://doi.org/10.5194/cp-11-1181-2015>
- Willard, D. A., Weimer, L. M., & Riegel, W. L. (2001). Pollen assemblages as palaeoenvironmental proxies in the Florida Everglades. *Review of Palaeobotany and Palynology*, 113, 213–235.
- Woodroffe, C. D., Rogers, K., McKee, K. L., Lovelock, C. E., Mendelssohn, I. A., & Saintilan, N. (2016). Mangrove sedimentation and response to relative sea-level rise. *Annual Review of Marine Science*, 8, 243–266. <https://doi.org/10.1146/annurev-marine-122414-034025>
- You, Y., Hubern, M., Müller, R. D., Poulsen, C. J., & Ribbe, J. (2009). Simulation of the Middle Miocene climate optimum. *Geophysical Research Letters*, 36, L04702. <https://doi.org/10.1029/2008GL036571>
- Zachos, J., Pagani, M., Sloan, L., Thomas, E., & Billups, K. (2001). Trends, rhythms, and aberrations in global climate 65 Ma to present. *Science*, 292, 686–693. <https://doi.org/10.1126/science.1059412>
- Zhu, J., Poulsen, C. J., Otto-Bliesner, B. L., Liu, Z., Brady, E. C., & Noone, D. C. (2020). Simulation of early Eocene water isotopes using an Earth system model and its implication for past climate reconstruction. *Earth and Planetary Science Letters*, 537, 116164. <https://doi.org/10.1016/j.epsl.2020.116164>

BIOSKETCH

Speranta-Maria Popescu is a palynologist involved in Cenozoic environmental reconstructions using pollen grains and dinoflagellate cysts, particularly in relation with climatic and geographical-geodynamic changes. After her Ph.D. and Accreditation to

supervise research, which she received from the Lyon 1 University, in 2001 and 2008, respectively, and postdoc at Woods Hole Oceanographic Institution, she started the GeoBioStratData Consulting company (www.geobiostratdata.com), which mainly specialises in biostratigraphical and palaeoenvironmental research projects with academic institutes and industrial companies.

Author Contributions: S.-M.P. & J.-P.S conceived the research, performed the Early Eocene pollen analyses, contributed to the Mid-Miocene pollen analyses and wrote the first draft of the paper; S.F. contributed by specifying the thermal requirements of the mangrove plant ecosystems and performed the climatic data-model comparison; M.B. and G.J.-M. provided several unpublished Mid-Miocene pollen analyses; C.R. helped conceive the research; L.L. contributed by estimating the palaeolatitude of the study locations. All the authors contributed to improve the manuscript.

SUPPORTING INFORMATION

Additional supporting information may be found online in the Supporting Information section.

How to cite this article: Popescu, S.-M., Suc, J.-P., Fauquette, S., Bessedik, M., Jiménez-Moreno, G., Robin, C., & Labrousse, L. (2021). Mangrove distribution and diversity during three Cenozoic thermal maxima in the Northern Hemisphere (pollen records from the Arctic–North Atlantic–Mediterranean regions). *Journal of Biogeography*, 48, 2771–2784. <https://doi.org/10.1111/jbi.14238>

Table S1.

Compiled mangrove pollen records at three thermal maxima (PETM, EECO, MMCO), referring to locations (exposed sections and boreholes) in Figures 2 and 3, with sources on bio- and chronostratigraphy and palaeolatitude estimates.

56 Ma Paleocene–Eocene thermal maximum (PETM): late Thanetian – early Ypresian.

Site No	Location (studied interval for holes)	Present latitude - longitude	Estimated N palaeolatitude	Mangrove pollen identified by	Mangrove taxa	References	
						Bio-chronostratigraphy	Pollen data
1	Site M0004A (382.44 mbsf) ¹	87°51'59.76"N 136°10'38.64"E	>76°	S.-M. Popescu J.-P. Suc	<i>Avicennia</i>	Suc et al. (2020)	
2	Faddeevsky Island Samples GS124-127 ²	76°06'23.30"N 141°49'01.70"E	80°	S.-M. Popescu J.-P. Suc	<i>Avicennia</i>	Suan et al. (2017)	
5	Site 918 hole D (1180.71-1180.49 mbsf)	63° 5'10.82"N 38°39'35.30"W	55°	S.-M. Popescu J.-P. Suc	<i>Avicennia</i> Rhizophoraceae <i>Xylocarpus</i> <i>Brownlowia</i>	Jolley (1998) Larsen et al. (1994) Wei (1998)	This work
7	Noirmoutier Samples 1-3	47° 0'39.99"N 2°13'11.04"W	35°	S.-M. Popescu J.-P. Suc	<i>Avicennia</i> Rhizophoraceae <i>Xylocarpus</i> <i>Nypa</i>	Ters (1978) Ollivier-Pierre (1980)	This work
8	Calavanté 1 (3350 m)	43°12'31.00"N 0°10'59.00"E	32°	S.-M. Popescu J.-P. Suc	<i>Avicennia</i> <i>Nypa</i>	Sztrákos et al. (1998)	This work
11	Site 547 hole A (279.53-279.31 mbsf)	33°46'50.40"N 9°20'58.80"W	19°	S.-M. Popescu J.-P. Suc	<i>Avicennia</i> Rhizophoraceae <i>Sonneratia</i> -type <i>Excoecaria</i> <i>Xylocarpus</i>	Hinz et al. (1984)	This work

Site Number (No) refers to Figure 2.

¹ Depth is indicated in mbsf (metres below sea level) for offshore boreholes.

² Samples are listed from base to top.

54–49 Ma Early Eocene climatic optimum (EECO): Ypresian.

Site No	Location (studied interval for holes)	Present latitude - longitude	Estimated N palaeolatitude	Mangrove pollen identified by	Mangrove taxa	References	
						Bio-chronostratigraphy	Pollen data
1	Site M0004A (318.86-282.05 mbsf)	87°51'59.76"N 136°10'38.64"E	>78°	S.-M. Popescu J.-P. Suc	<i>Avicennia</i>	Backman et al. (2006)	Suc et al. (2020)
3	Caribou Hills Samples 12-18	68°45'0.07"N 134°14'0.00"W	73°	S.-M. Popescu J.-P. Suc	<i>Avicennia</i>	Salpin et al. (2019)	
4	Site 343 (214.30-213.99 mbsf)	68°43'13.07"N 5°46'21.54"E	58°	S.-M. Popescu J.-P. Suc	<i>Avicennia</i> Rhizophoraceae <i>Xylocarpus</i> <i>Scyphiphora</i> <i>Excoecaria</i>	Müller (2007) Schrader et al. (2007)	This work
5	Site 918 hole D (1158.21-1156.71 mbsf)	63° 5'10.82"N 38°39'35.30"W	55°	S.-M. Popescu J.-P. Suc	<i>Avicennia</i> Rhizophoraceae <i>Sonneratia</i> -type <i>Brownlowia</i> <i>cf. Heritiera</i>	Larsen et al. (1994) Wei (1998)	This work
6	Kallo 027E148 (286.50-239 m)	51°15'8.25"N 4°17'38.21"E	40°	S.-M. Popescu J.-P. Suc	<i>Avicennia</i> Rhizophoraceae <i>Sonneratia</i> -type <i>Nypa</i>	Roche (1973) Steurbaut (2006)	This work
9	Morlaàs 1 (1462-1083 m)	43°19'42.00"N 0°14'17.00"W	32°	S.-M. Popescu J.-P. Suc	<i>Avicennia</i> Rhizophoraceae <i>Sonneratia</i> -type <i>Nypa</i> <i>Pelliciera</i> <i>Xylocarpus</i>	Sztrákos et al. (1998)	This work
10	Gan Samples 1-2	43°13'54.20"N 0°23'45.80"W	33°	S.-M. Popescu J.-P. Suc	<i>Avicennia</i> Rhizophoraceae <i>Sonneratia</i> -type <i>Aegialitis</i> <i>Nypa</i>	Alimen et al. (1963)	This work

Site Number (No) refers to Figure 2.

17–14 Ma Mid-Miocene climatic optimum (MMCO): late Burdigalian – Langhian.

Site No	Location (studied interval for boreholes)	Present latitude - longitude	Estimated N palaeolatitude	Mangrove pollen identified by	Mangrove taxa	References	
						Bio-chronostratigraphy	Pollen data
1	Göllersdorf Samples 1-8	48°30'06.79"N 16°07'32.44"E	45°	G. Jiménez-Moreno	<i>Avicennia</i>	Roetzel et al. (1999)	Jiménez-Moreno et al. (2008)
2	Herend 46 (79-78 m)	47°07'58.43"N 17°45'15.99"E	43°	J.-P. Suc	<i>Avicennia</i>	Nagy & Kokay (1991)	
3	Balgarevo C136A (300-270 m)	43°26'01.78"N 28°24'45.12"E	41°	J.-P. Suc	<i>Avicennia</i>	Ivanov et al. (2007)	Ivanov et al. (2007, 2015)
4	Les Mées 1 (1420-1060 m) Châteauredon	44°01'00.84" N 5°59'14.50"E 44°01'17.12"N 6°13'50.12"E	40.5°	G. Jiménez-Moreno	<i>Avicennia</i>	Dubois & Curnelle (1978) Besson et al. (2005)	Jiménez-Moreno & Suc (2007)
5	Estagel Sampes 4-10 Bayanne Samples 1-3	43°31'06.61"N 4°59'52.09"E 43°31'56.36"N 4°58'48.95"E	40°	G. Jiménez-Moreno	<i>Avicennia</i>	Besson et al. (2005)	Jiménez-Moreno & Suc (2007)
6	Narbonne V. Hugo College (23-11 m) Lespignan II Montady Saint-Géniès Montagnac Mèze Loupian Issanka Poussan Montbazin	from 43°11'34.75"N 3°00'36.88"E to 43°31'24.40"N 3°42'02.90"E	39.5°	M. Bessedik	<i>Avicennia</i>	Aguilar (1981) Cappetta (1970) Magné (1978b) Bessedik (1985)	Bessedik (1984, 1985)
7	La Rierussa Samples 1-16 Sant Pau d'Ordal	41°23'04.77"N 1°48'41.96"E 41°23'04.77"N 1°48'04.42"E	37.5°	G. Jiménez-Moreno M. Bessedik	<i>Avicennia</i>	Magné (1978a) Bessedik (1985)	Bessedik & Cabrera (1985) Jiménez-Moreno & Suc (2007) Jiménez-Moreno et al. (2010)
8	Kultak	37°04'42.27"N 27°56'24.59"E	33°	M.S. Kayseri-Özer	<i>Avicennia</i>	Kayseri-Özer (2014)	
9	Alboran A1 (1193-1163 mbsf)	36°38'00"N 4°13'23"W	33°	G. Jiménez-Moreno	<i>Avicennia</i>	Jiménez-Moreno (2005)	Jiménez-Moreno & Suc (2007) Jiménez-Moreno et al. (2010)
10	Laborde 1D (180-160 m)	43°55'48.825"N 1°04'53.459"W	40°	S.-M. Popescu J.-P. Suc	None	Órtiz et al. (2020)	This work
11	Bignona (149-135 m)	12°46'41.39"N 16°15'26.54"W	8°	J. Médus	<i>Rhizophora</i>	Médus (1975)	
12	Well M1 (2091-2012 m)	ca. 11°N, ca. 2°E	2°	E.U. Durugbo & M.A. Olayiwola	<i>Avicennia</i> <i>Rhizophora</i>	Durugbo & Olayiwola (2017)	
13	Site M0027 (250-200 mbsf)	39°38'02.76"N 73°37'18.06"W	37°		None	Mountain et al. (2010)	Kotthoff et al. (2014)
14	Alum Bluff	30°28'08"N 84°59'10"W	28.5°		None	Bryant et al. (1992)	Corbett (2004) Jarzen et al. (2010)
15	La Herradura	17°20'57.94"N 93°33'18.96"W	15°	R. Palacios Chavez	<i>Rhizophora</i> <i>Pelliciera</i> <i>Nypa</i>	Palacios Chavez & Rzedowski (1993)	
16	Lower Apaporis River	0°19'57.26"S 70°07'04.82"W	-3.5°	C. Hoorn	<i>Rhizophora</i>	Hoorn (2006)	

Site Number (No) refers to Figure 3.

Chronology

As indicated above, a relatively rough age model is provided by biostratigraphy (planktonic foraminifera and/or calcareous nannofossils). A recent oxygen isotope curve is used as reference of global climate variations (Fig. S1; Westerhold et al., 2020). This curve comes from a Cenozoic global dataset based on benthic foraminifera with a sampling interval of 2 to 4.4 kyr. The blue curve is a smoothed curve over 20 kyr and the red curve over 1 Myr. They respectively express different rhythms in temperature variability. The variations observed in pollen records (Figs. 4–6) are mainly interpreted as variation in temperature for the PETM, EECO and Göllersdorf during the MMCO because the pollen diagrams evidence humid conditions (prevalent thermophilous plants, weakness of herbs). For the other MMCO locations, the variations in pollen records are both interpreted as temperature and precipitation variations (forest humid and warmer phases marked by abundant thermophilous

trees opposed to herbaceous drier and less warm phases marked by abundant herbs). According to the time interval represented by each pollen record and according to the number of samples studied within this interval (i.e., the time resolution of each record), we tentatively correlate the pollen variations observed with either the blue curve either the red curve (Fig. S1), following the principles of climatostratigraphy described by Suc (1984), Suc et al. (2018) and Suc et al. (2020).

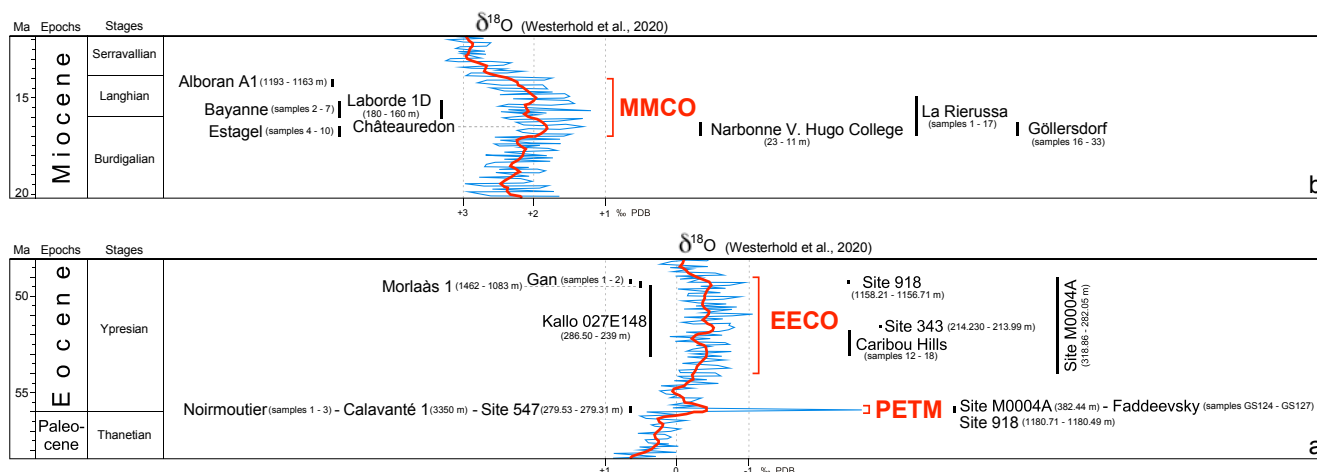


Figure S1. Climatostratigraphic correlations of the studied pollen records with the reference oxygen isotope curve: a, during the PETM and EECO; b, during the MMCO. Explanations are given above.

References.

- Aguilar, J.-P. (1981). *Evolution des rongeurs miocènes et paléogéographie de la Méditerranée occidentale*. PhD thesis, University of Montpellier, 203 p.
- Alimen, H., Crouzel, F., Debourle, A., Fourmentrau, J., Henry, J., Cuvillier, J., Delmas, M., Deloffre, R., & Delbushaye, J. (1963). Pau. Carte géologique de la France à 1/50000^{ème}, 1029, Bureau de Recherches Géologiques et Minières.
- Backman, J., Moran, K., McInroy, D. B., Mayer, L. A., & the Expedition 302 Scientists (2006). Sites M0001–M0004. *Proceedings of the Integrated Ocean Drilling Program*, 302, 1–169.
- Bessedik, M. (1984). The early Aquitanian and upper Langhian-lower Serravallian environments in the northwestern Mediterranean region. *Paléobiologie continentale*, 14(2), 153–179.
- Bessedik, M. (1985). Reconstitution des environnements miocènes des régions nord-ouest méditerranéennes à partir de la palynologie. PhD thesis, University of Montpellier, 162 p.
- Bessedik, M., & Cabrera, L. (1985). Le couple récif-mangrove à Sant Pau d'Ordal (Vallès-Pénédes, Espagne), témoin du maximum transgressif en méditerranée nord occidentale (Burdigalien supérieur – Langhien inférieur). *Newsletters on Stratigraphy*, 14(1), 20–35.
- Besson, D., Parize, O., Rubino, J.-L., Aguilar, J.-P., Aubry, M.-P., Beaudoin, B., Berggren, W. A., Clauzon, G., Crumeyrolle, P., Dexcoté, Y., Fiet, N., Iaccarino, S., Jiménez-Moreno, G., Laporte-Galaa, C., Michaux, J., von Salis, K., Suc, J.-P., Reynaud, J.-Y., & Wernli, R. (2005). Un réseau fluvial d'âge burdigalien terminal dans le sud-est de la France : remplissage, extension, âge, implications. *Comptes-Rendus Geoscience, Stratigraphie, Géomorphologie*, 337, 1045–1054.
- Bryant, J. D., MacFadden, B. J., Mueller, P. A. (1992). Improved chronologic resolution of the Hawthorn and the Alum Bluff Groups in northern Florida: implications for Miocene chronostratigraphy. *Geological Society of America Bulletin*, 104, 208–218.
- Cappetta, H. (1970). Les Sélaciens du Miocène de la région de Montpellier. *Palaeovertebrata*, Mémoire extraordinaire, 4–11 & 120–123.

- Corbett, S.L. (2004). The middle Miocene Alum Bluff flora, Liberty County, Florida. Master thesis, University of Florida, 97 p.
- Dubois, P., & Curnelle, R. (1978). Résultats apportés par le forage Les Mées 1 sur le plateau de Valensole (Alpes-de-Haute-Provence). *Comptes-Rendus sommaires de la Société géologique de France*, 4, 181–184.
- Durugbo, E.U., & Olayiwola, M.A. (2017). Palynological dating and palaeoenvironments of the M1 well, Middle Miocene, Niger Delta, Nigeria. *Palaeontologia africana*, 52, 46–57.
- Fauquette, S., Suc, J.-P., Médail, F., Muller, S. D., Jiménez-Moreno, G., Bertini, A., Martinetto, E., Popescu, S.-M., Zheng, Z., & de Beaulieu, J.-L. (2018). The Alps: A geological, climatic and human perspective on vegetation history and modern plant diversity. In “Mountains, climate, and biodiversity”, Hoorn, C., Perrigo, A., Antonelli, A., eds., Wiley, 27, 413–428.
- Hinz, K., Winterer, E. L., & the Shipboard Scientific Party (1984). Site 547. *Proceedings of the Deep Sea Drilling Project, Initial Reports*, 79, 223–361.
- Hoorn, C. (2006). Mangrove forests and marine incursions in Neogene Amazonia (Lower Apaporis River, Colombia). *Palaios*, 21(2), 206–219.
- Ivanov, D., Ashraf, A. R., & Mosbrugger, V. (2007). Late Oligocene and Miocene climate and vegetation in the Eastern Paratethys area (northeast Bulgaria) based on pollen data. *Palaeogeography, Palaeoclimatology, Palaeoecology*, 255, 342–360.
- Ivanov, D., Bozukov, V., & Utescher, T. (2015). On the presence of mangrove elements in the Cenozoic vegetation of Bulgaria. 10th Romanian Symposium on Palaeontology, Abstract Volume, 40–41.
- Jarzen, D. M., Corbett, S. L., & Manchester, S. R. (2010). Palynology and paleoecology of the Middle Miocene Alum Bluff flora, Liberty County, Florida, USA. *Palynology*, 34, 261–286.
- Jiménez-Moreno, G. (2005). Utilización del análisis polínico para la reconstrucción de la vegetación, clima y estimación de paleoaltitudes a lo largo de arco alpino europeo durante el Mioceno (21–8 Ma). PhD thesis, C. Bernard-Lyon 1 University and Grenade University.
- Jiménez-Moreno, G., Fauquette, S., & Suc, J.-P. (2008). Vegetation, climate and palaeoaltitude reconstructions of the Eastern Alps during the Miocene based on pollen records from Austria, Central Europe. *Journal of Biogeography*, 35, 1638–1649.
- Jiménez-Moreno, G., Fauquette, S., & Suc, J.-P. (2010). Miocene to Pliocene vegetation reconstruction and climate estimates in the Iberian Peninsula from pollen data. *Review of Palaeobotany and Palynology*, 162, 403–415.
- Jiménez-Moreno, G., Popescu, S.-M., Ivanov, D., & Suc, J.-P. (2007). Neogene flora, vegetation and climate dynamics in Central Eastern Europe according to pollen records. In “Deep-Time Perspectives on Climate Change. Marrying the Signal from Computer Models and Biological Proxies”, Williams M., Haywood A., Gregory J., Schmidt D. N. eds., The Micropaleontological Society, *The Geological Society, London, Special Publications*, 393–406.
- Jiménez-Moreno, G., & Suc, J.-P. (2007). Middle Miocene latitudinal climatic gradient in Western Europe: Evidence from pollen records. *Palaeogeography, Palaeoclimatology, Palaeoecology*, 253, 224–241.
- Jolley, D. W. (1998). Early Eocene palynofloras from Holes 915A, 916A, 917A, and 918D, East Greenland. *Proceedings of the Ocean Drilling Program, Scientific Results*, 152, 221–231.
- Kayseri-Özer, M. S. (2014). Spatial distribution of climatic conditions from the Middle Eocene to Late Miocene based on palynoflora in Central, Eastern and Western Anatolia. *Geodinamica Acta*, 26, 122–157.
- Kotthoff, U., Greenwood, D. R., McCarthy, F. M. G., Müller-Navarra, K., Prader, S., & Hesselbo, S. P. (2014). Late Eocene to middle Miocene (33 to 13 million years ago) vegetation and climate development on the North American Atlantic Coastal Plain (IODP Expedition 313, Site M0027). *Climate of the Past*, 10, 1523–1539.

- Larsen, H. C., Saunders, A. D., Clift, P. D., & the Shipboard Scientific Party (1994). Site 918. *Proceedings of the Ocean Drilling Program, Initial Reports*, 152, 177–256.
- Magné, J. (1978a). *Etudes microstratigraphiques sur le Néogène de la Méditerranée nord-occidentale. Les bassins néogènes catalans*. Editions du C.N.R.S., Paris, 259 p.
- Magné, J. (1978b). *Etudes microstratigraphiques sur le Néogène de la Méditerranée nord-occidentale. Le Néogène du Languedoc méditerranéen*. Laboratoire de Géologie Méditerranéenne, University p. Sabatier, Toulouse, 435 p.
- Médus, J. (1975). Palynologie de sediments tertiaries du Sénégal méridional. *Pollen et Spores*, 17(4), 545–608.
- Mountain, G. S., Proust, J.-N., McInroy, D., Cotterill, C., & the Expedition 313 Scientists (2010). Site M0027. *Proceedings of the Integrated Ocean Drilling Program, Expedition Reports*, 313, 1–148.
- Müller, C. (2007). Tertiary and Quaternary calcareous nannoplankton in the Norwegian–Greenland Sea, DSDP, Leg 38. *Proceedings of the Deep Sea Drilling Project, Scientific Reports*, 38, 823–841.
- Nagy, E., & Kóky, J. (1991). Middle Miocene mangrove vegetation in Hungary. *Acta Geologica Hungarica*, 34(1–2), 45–52.
- Ollivier-Pierre M.-F. (1980). Etude palynologique (spores et pollens) de gisements paléogènes du Massif Américain. Stratigraphie et paléogéographie. *Mémoires de la Société géologique et minéralogique de Bretagne*, 25, 1–239.
- Ortiz, A., Guillocheau, F., Lasseur, E., Briais, J., Robin, C., Serrano, O., & Fillon, C. (2020). Sediment routing system and sink preservation during the post-orogenic evolution of a retroforeland basin: the case example of the North Pyrenean (Aquitaine, Bay of Biscay) Basins. *Marine and Petroleum Geology*, 112, 104085.
- Palacios Chavez, R., & Rzedowski, J. (1993). Estudio palinológico de las floras fosiles del Miocene inferior y principios del Miocene medio de la region de Pichucalco, Chiapas, Mexico. *Acta Botánica Mexicana*, 24, 1–96.
- Roche, E. (1973). Etude palynologique des couches yprésiennes du sondage de Kallo. *Bulletin de la Société belge de Géologie, Paléontologie, Hydrologie*, 82(4), 487–495.
- Roetzel, R., Cicha, I., Stojaspal, F., Decker, K., Wimmer-Frey, I., Ottner, F., & Papp, H. (1999). Göllersdorf – Zieglei und Tombergau Wienerberger. In “Arbeitstagung Geologische Bundesanstalt”, Roetzel, R., ed., Geologische Karten ÖK 9 Retz und ÖK 22 Hollabrunn, Geologische Bundesanstalt, Vienna, 335–341.
- Salpin, M., Schnyder, J., Baudin, F., Suan, G., Suc, J.-P., Popescu, M.-S., Fauquette, S., Reinhardt, L., Schmitz, & M., Labrousse, L. (2019). Evidence for subtropical warmth in Canadian Arctic (Beaufort-Mackenzie, Northwest Territories, Canada) during the early Eocene. In ‘Circum-Arctic Structural Events: Tectonic Evolution of the Arctic Margins and Trans-Arctic Links with Adjacent Orogens’, *Geological Society of America Special Paper* 541, 27, 637–664.
- Schrader, H.-J., Bjørklund, K., Manum, S., Martini, E., & van Hinte, J. (2007). Cenozoic biostratigraphy, physical stratigraphy and paleoceanography in the Norwegian–Greenland Sea, DSDP Leg 38 Paleontological synthesis. *Proceedings of the Deep Sea Drilling Project, Scientific Reports*, 38, 1197–1211.
- Sturbaut, E. (2006). Ypresian. *Geologica Belgica*, 9(1–2), 73–93.
- Suan, G., Popescu, S.-M., Suc, J.-P., Schnyder, J., Fauquette, S., Baudin, F., Yoon, D., Piepjohn, K., Sobolev, N., & Labrousse, L. (2017). Subtropical climate conditions and mangrove growth in Arctic Siberia during the early Eocene. *Geology*, 45, 6, 539–542.
- Suc, J.-P. (1984). Origin and evolution of the Mediterranean vegetation and climate in Europe. *Nature*, 307, 429–432.
- Suc, J.-P., Fauquette, S., Popescu, S.-M., & Robin, C. (2020). Subtropical mangrove and evergreen forest reveal Paleogene terrestrial climate and physiography at the North Pole. *Palaeogeography, Palaeoclimatology, Palaeoecology*, 551, 109755.

- Suc, J.-P., Popescu, S.-M., Fauquette, S., Bessedik, M., Jiménez-Moreno, G., Bachiri Taoufiq, N., Zheng, Z., & Médail, F. (2018). Reconstruction of Mediterranean flora, vegetation and climate for the last 23 million years based on an extensive pollen dataset. *Ecologia mediterranea*, 44(2), 53–85.
- Sztràkos, K., Gély, J.-P., Blondeau, A., & Müller, C. (1998). L'Eocène du bassin sud-aquitain: lithostratigraphie, biostratigraphie et analyse séquentielle. *Géologie de la France*, 4 57–105.
- Ters M. (1978). Ile-de-Noirmoutier – Pointe-de-St-Gildas. Carte géologique de la France à 1/50000^{ème}, 506–533, Bureau de Recherches Géologiques et Minières. Notice, 35 p.
- Wei, W. (1998). Calcareous nannofossils from the southeast Greenland Margin: biostratigraphy and paleoceanography. *Proceedings of the Ocean Drilling Program, Scientific Results*, 152, 147–160.
- Westerhold, T., Marwan, N., Drury, A.J., Liebrand, D., Agnini, C., Anagnostou, E., Barnet, J.S.K., Bohaty, S.M., De Vleeschouwer, D., Florin, D., Lauretano, V., Littler, K., Lourens, L.J., Lyle, M., Pälike, H., Röhl, U., Tian, J., Wilkens, R.H., Wilson, P.A., Zachos, J.C. (2020). An astronomically dated record of Earth's climate and its predictability over the last 66 million years. *Science*, 369, 1383–1387.

Table S2. Listing of taxa constituting the ecological groups of plants used for the synthetic pollen diagrams, distributed by locations with respect to PETM, EECO and MMCO, respectively.

The suffix '-type' is used to indicate that the concerned pollen morphology exists in several taxa (species or genera). The prefix 'cf.' means that the selected taxon has the nearest morphology with the fossil pollen after comparison with pollen of modern species or genera.

Ecological groups of plants	Taxa	PETM locations					EECO locations					MMCO locations									
		1	2	5	7	8	11	1	3	4	5	6	9	10	1	4	5	6	7	9	10
Avicennia	<i>Avicennia</i>	x	x	x	x	x	x	x	x	x	x	x	x	x	x	x	x	x	x	x	x
Other mangrove trees and shrubs	cf. <i>Aegialitis</i>													x							
	<i>Brownlowia</i>			x							x										
	<i>Excoecaria</i>						x			x											
	cf. <i>Heritiera</i>										x										
	<i>Nypa</i>				x	x						x	x	x							
	<i>Pelliciera</i>												x								
	Rhizophoraceae			x	x		x			x	x	x	x	x							
	<i>Scyphiphora</i>										x										
	<i>Sonneratia</i> type						x				x	x	x	x							
<i>Xylocarpus</i>			x	x		x			x			x									
Other megathermal plants	Acanthaceae			x								x					x		x		
	<i>Alchornea</i>												x				x		x		
	<i>Amanoa</i>									x			x	x							
	<i>Bombax</i> type			x			x						x				x		x		
	cf. <i>Bridelia</i>											x									
	<i>Buxus bahamensis</i> type			x	x					x		x	x	x			x	x			
	<i>Canthium</i> type											x	x								
	cf. <i>Corypha</i>													x							
	<i>Croton</i>									x							x		x	x	
	<i>Dodonaea</i>						x				x	x	x	x				x		x	
	cf. <i>Drypetes</i>						x							x							
	Euphorbiaceae	x		x	x		x	x			x		x	x	x	x		x	x	x	x
	<i>Fothergilla</i>										x						x		x		
	cf. <i>Gordonia</i>									x											
	<i>Grewia-Corchorus</i>												x							x	
	Icacinaceae	x										x									
	cf. <i>Lasianthus</i>													x							
	Leguminosae Caesalpinioideae				x	x						x	x	x			x			x	x
	Leguminosae Mimosoideae			x													x			x	x
	Malpighiaceae																				x
	<i>Mappianthus</i>													x				x		x	
	Melastomataceae												x				x	x	x		
	Meliaceae				x								x	x	x	x	x	x	x	x	
	<i>Morinda-Randia</i> type												x								
	cf. <i>Parsonsia</i>												x								
	Passifloraceae			x	x												x			x	
	<i>Phyllostylon</i>				x						x	x									
<i>Prosopis</i>																				x	
Sapindaceae						x							x	x							
cf. <i>Sapium</i>														x							
Simaroubaceae				x																	
<i>Sindora</i>					x	x															
Theaceae				x													x				
Tiliaceae																		x			
Mega-mesothermal plants	cf. <i>Acanthopanax</i>												x								
	Agavaceae																			x	
	<i>Alangium</i>													x							
	cf. <i>Alfaroa</i>	x		x	x	x	x	x			x	x	x								
	Arecaceae	x	x	x	x	x		x	x	x	x	x	x	x	x	x	x	x	x	x	x
cf. <i>Beaumontia</i>					x																

Ecological groups of plants	Taxa	PETM locations					EECO locations					MMCO locations									
		1	2	5	7	8	11	1	3	4	5	6	9	10	1	4	5	6	7	9	10
Mega-mesothermal plants	<i>Castanopsis-Lithocarpus</i>	x	x	x	x			x	x	x	x	x	x		x		x	x	x		x
	<i>Casuarina</i>			x	x		x	x		x	x										
	Celastraceae		x				x											x	x		x
	<i>Ceratonia</i>																	x			
	Chloranthaceae																	x			
	<i>Cissus</i>			x						x	x			x	x						x
	<i>Cordyline</i>																			x	
	Cornaceae																			x	
	cf. <i>Corylopsis</i>																			x	
	<i>Craigia</i>			x	x					x	x		x	x							
	Cupressaceae (former Taxodiaceae type)	x	x	x	x	x	x	x	x	x	x	x	x	x	x	x	x	x	x	x	x
	Cyrillaceae-Clethraceae				x				x	x			x			x		x		x	
	<i>Dacrydium</i>									x											
	<i>Decodon</i>		x				x						x	x							
	<i>Dicoryphe</i>				x					x											
	<i>Diplodiscus</i>				x																
	<i>Distylium</i>	x	x	x	x		x		x	x	x	x	x	x	x	x		x	x	x	x
	<i>Embolanthera</i>			x	x				x		x									x	
	<i>Engelhardia</i>	x	x	x	x	x	x		x	x	x	x	x	x	x	x	x	x	x	x	x
	<i>Eustigma</i>			x			x													x	
	Hamamelidaceae																x	x	x	x	x
	<i>Hamamelis</i>																			x	x
	<i>Ilex floribunda</i> type				x				x			x		x						x	
	<i>Ipomoea</i>											x									
	<i>Itea</i>										x										
	Lauraceae															x					
	<i>Leea</i>		x		x						x	x	x		x					x	
	<i>Liriodendron</i>				x																
	Loranthaceae														x					x	
	<i>Loropetalum</i>		x										x	x	x					x	
	<i>Ligustrum</i>															x				x	x
	cf. <i>Lysidice</i>				x																
	<i>Magnolia</i>				x																
	<i>Matudaea</i>								x	x											
	Menispermaceae		x		x		x						x						x	x	x
	<i>Microtropis fallax</i>				x															x	x
	<i>Mussaenda</i> type													x	x	x				x	x
	<i>Myrica</i>	x	x		x				x	x	x		x	x	x	x	x	x	x	x	x
	<i>Nolina</i>													x							
	<i>Nyssa</i>		x	x	x	x			x	x	x	x	x	x					x	x	x
	<i>Nyssa</i> cf. <i>sinensis</i>		x	x					x	x		x	x								
	<i>Olea</i>				x								x			x	x	x	x	x	x
	<i>Phillyrea</i>																			x	x
	<i>Pistacia</i>																			x	
	<i>Platycarya</i>			x	x	x			x	x			x	x	x	x				x	x
<i>Rhamnus</i>																			x		
<i>Rhodoleia</i>		x	x			x		x		x	x	x							x	x	
<i>Rhoiptelea</i>				x															x		
<i>Rhus</i> cf. <i>cotinus</i>																			x	x	
cf. <i>Ricinus</i>			x	x					x			x							x	x	
Rubiaceae										x	x	x		x	x	x	x	x	x	x	
Sapotaceae		x		x	x						x	x	x	x					x	x	
<i>Sciadopitys</i>					x			x	x	x	x	x							x		
<i>Sequoia</i> type																			x		
Styracaceae																					
<i>Symplocos</i>		x								x		x							x	x	
<i>Taxodium</i> type	x	x	x	x	x	x		x	x	x	x	x	x	x	x	x	x			x	
cf. <i>Trichocladus</i>																				x	
<i>Uncaria</i> type		x								x	x		x	x						x	

Ecological groups of plants	Taxa	PETM locations					EECO locations					MMCO locations										
		1	2	5	7	8	11	1	3	4	5	6	9	10	1	4	5	6	7	9	10	
Mesothermal plants	<i>Acer</i>	x	x	x			x	x	x	x	x		x	x	x	x		x	x	x	x	x
	<i>Aesculus</i>		x																			
	<i>Alnus</i>	x	x	x			x	x	x	x	x	x		x	x	x		x	x	x	x	x
	Anacardiaceae							x			x							x	x			
	Araliaceae								x													
	<i>Betula</i>							x	x				x	x				x	x			x
	<i>Buxus sempervirens</i> type		x													x	x	x	x	x		x
	Caprifoliaceae																				x	
	<i>Carpinus</i>	x	x	x				x	x	x				x	x	x		x	x	x		
	<i>Carya</i>	x	x	x	x	x	x	x	x	x	x	x	x			x	x	x	x	x	x	x
	<i>Celtis</i>			x	x		x	x		x	x					x		x	x	x		
	<i>Corylus</i>																			x		
	Ericaceae		x		x			x	x	x	x	x				x	x	x	x	x	x	x
	<i>Erica cf. terminalis</i>																					x
	<i>Eucommia</i>			x	x			x	x		x	x		x				x	x			
	<i>Fraxinus</i>							x			x											
	<i>Hedera</i>			x							x							x			x	x
	<i>Ilex</i>															x		x		x	x	
	<i>Juglans</i>				x			x								x		x	x	x		
	<i>Liquidambar</i>		x				x	x	x	x	x					x	x	x	x	x		
	<i>Lonicera</i>																				x	
	<i>Nothapodytes</i>				x																	
	Oleaceae															x	x	x	x	x		
	<i>Ostrya</i>				x			x	x			x										x
	<i>Parrotia cf. persica</i>			x	x		x	x				x				x		x	x	x		
	<i>Parrotiopsis cf. jacquemontiana</i>							x				x										x
	<i>Parthenocissus</i>						x				x	x				x		x		x		
	<i>Parthenocissus cf. henryana</i>		x					x	x			x										
	<i>Phelline</i>				x																	
	<i>Platanus</i>		x													x						
	<i>Populus</i>	x	x		x			x	x					x				x	x			x
	<i>Pterocarya</i>		x	x	x	x	x	x	x	x	x	x				x	x	x	x			
	<i>Quercus</i>	x	x	x	x		x	x	x	x	x	x	x	x	x	x	x	x	x	x	x	x
	<i>Quercus ilex</i> type															x	x		x	x		
	Rhamnaceae		x					x	x	x	x							x	x			
	<i>Rhus</i>				x		x					x	x	x	x	x		x		x	x	
	<i>Salix</i>			x	x		x	x	x	x	x	x		x	x	x	x	x	x	x	x	x
	<i>Sambucus</i>						x															
	<i>Tamarix</i>				x													x	x	x		
	<i>Tilia</i>	x		x	x			x	x	x						x		x	x	x		
<i>Ulmus</i>	x	x	x	x	x	x	x	x	x	x	x	x	x	x			x	x			x	
<i>Ulmus-Zelkova</i>																			x			
<i>Viburnum</i>																	x		x			
<i>Vitis</i>		x													x		x					
<i>Zelkova</i>	x	x					x	x		x		x	x	x	x	x	x	x	x		x	
<i>Pinus</i> + indeterminable Pinaceae	diplostellate type	x	x	x	x	x	x		x	x	x	x	x	x	x	x	x	x	x	x	x	
	haplostellate type		x					x									x					
	haploxylon type								x													
Meso-microthermal plants	<i>Cathaya</i>		x	x	x	x	x	x	x	x	x	x			x	x	x	x	x	x	x	
	<i>Cedrus</i>			x	x			x		x	x						x				x	
	<i>Fagus</i>							x	x	x					x		x		x		x	
	<i>Podocarpus</i>			x		x	x	x	x	x	x	x	x									
	<i>Tsuga</i>		x					x	x			x					x	x				
Microthermal plants	<i>Abies</i>							x	x	x					x		x				x	
	<i>Picea</i>		x			x		x	x	x	x	x			x		x				x	

Ecological groups of plants	Taxa	PETM locations					EECO locations					MMCO locations										
		1	2	5	7	8	11	1	3	4	5	6	9	10	1	4	5	6	7	9	10	
Elements without significance	<i>Aglaoreidia</i>											x										
	cf. <i>Alyxia</i>				x	x						x	x	x								
	Apocynaceae												x	x								
	Convolvulaceae																	x				
	cf. Cucurbitaceae													x								
	<i>Dolichandrone</i>			x																		
	Normapolles				x			x	x			x	x	x								
	Ranunculaceae	x		x	x			x	x	x		x		x			x				x	x
	Rosaceae	x						x	x			x		x	x	x	x			x	x	
	Rutaceae	x		x									x	x	x		x			x	x	
	<i>Sanguisorba</i> type											x										
	Solanaceae																	x				
	<i>Tricolporopollenites sibiricum</i>														x		x			x		
	Unidentified pollen grains	x	x	x	x	x		x	x	x	x	x	x	x			x	x	x	x	x	x
Vitaceae																	x					
Cupressaceae <i>p.p.</i>	<i>Cupressus-Juniperus</i> type	x	x	x	x	x	x	x	x	x	x	x	x	x		x	x	x	x	x	x	
Herbaceous plants	<i>Alisma</i>						x	x	x	x		x										
	Amaranthaceae				x									x	x	x	x	x	x	x		
	Apiaceae													x				x	x	x		
	<i>Aquilegia</i> type	x																				
	<i>Artemisia</i>	x	x					x						x		x		x				
	<i>Asphodelus</i>					x																
	Boraginaceae																x					
	Brassicaceae																x		x			
	<i>Bupleurum</i>																	x				
	<i>Calligonum</i>						x															
	Campanulaceae	x	x		x	x		x				x	x							x		
	Caryophyllaceae													x	x				x	x		
	<i>Cephalanthus</i>											x									x	
	Cistaceae																x	x	x			
	<i>Cistus</i>																	x				
	Compositae Asteroideae			x	x		x				x	x	x			x	x	x	x	x		
	Compositae Cichorioideae							x						x	x		x	x	x	x		
	<i>Convolvulus</i>				x			x				x						x	x		x	
	Crassulaceae							x														
	<i>Cuphea</i>			x																		
	Cyperaceae	x		x				x	x			x		x		x					x	
	<i>Diodia</i> type							x														
	<i>Ephedra</i>														x				x	x		
	<i>Erodium</i>																x		x			
	<i>Euphorbia</i>	x						x														
	<i>Filipendula</i>																x					
	<i>Galium</i>																x					
	Gentianaceae							x		x												
	Geraniaceae													x					x			
	<i>Geranium</i>	x																				
	<i>Gunnera</i>												x									
	<i>Helianthemum</i>										x							x		x		
	<i>Hyoscyamus</i>																	x				
	Leguminosae Papilionideae							x					x	x		x	x	x	x	x		
	Liliaceae													x		x		x	x			
	<i>Linum</i>																		x		x	
	cf. <i>Lobelia</i>											x										
	<i>Lygeum</i>																				x	
	<i>Lythraceae</i>																	x				
	Malvaceae																	x	x			
<i>Melilotus</i> type										x												
Menyanthaceae	x	x				x	x	x		x												
<i>Mercurialis</i>				x													x		x	x		
Aquatic monocotyledon					x							x					x					

Ecological groups of plants	Taxa	PETM locations					EECO locations					MMCO locations										
		1	2	5	7	8	11	1	3	4	5	6	9	10	1	4	5	6	7	9	10	
Herbaceous plants	<i>Myriophyllum</i>				x			x				x										
	<i>Nitraria</i>										x									x		
	Nymphaeaceae																		x			
	Oenotheraceae		x						x			x			x							
	Papaveraceae		x			x	x		x	x		x	x									
	<i>Plantago</i>								x									x	x	x	x	x
	Plumbaginaceae																			x	x	x
	Poaceae			x		x	x						x	x			x	x	x	x	x	x
	Polygonaceae																		x		x	
	<i>Polygonum</i>								x													
	<i>Polygonum aviculare</i> type								x													
	<i>Potamogeton</i>				x	x							x	x						x	x	
	Primulaceae								x													
	Resedaceae			x						x	x	x	x	x								x
	Restionaceae			x	x	x				x		x	x								x	
	<i>Restio</i>				x	x						x	x									
	<i>Rumex</i>				x		x			x	x									x	x	x
	Saxifragaceae													x								
	<i>Sparganium</i>				x																x	x
	<i>Thalictrum</i>										x										x	x
<i>Typha</i>																				x	x	
Urticaceae		x				x				x	x	x	x	x					x	x	x	
Valerianaceae					x				x												x	

The pollen data used for the PETM and EECO result from recent analyses because of a noteworthy evolution in Paleogene palynology. The pollen records used for MMCO are relatively recent and homogenous enough in terms of botanical identifications.

Botanical identification of pollen grains

The rarely used technique of mounting the residue in glycerol allows some mobility of the pollen grains so their different sides can be examined, thus facilitating their botanical identification. Analyses were made using a light microscope at 200x magnification, and each pollen grain was identified at 1,000x magnification.

Aiming to optimize reliability of pollen analysis, we perform appropriate techniques (see the chapter ‘Material and methods’ of the main text and we follow an accurate nomenclature in pollen morphology (Punt et al., 2007) for understanding shape, structure, aperture(s) and ornamentation, according to the LO-analysis (*Lux* = light vs. *Obscuritas* = darkness) technique of observation at the transmitted light microscope (TLM) (Erdtman, 1952). Scanning electronic microscope (SEM) has also been used to check some of the pollen characters, particularly those perceptible in surface, such as shape and ornamentation. Information on the present-day accepted botanical taxa and synonymies comes from The Plant List (2013). Most of the pollen photographs come from specimens from the ISEM collection (website: data.oreme.org), some others come from the GeoBioStratData private collection.

Below, we provide an accurate description, illustrated by photographs, of some critical pollen grains benefiting from a botanical identification, which belong to plants of the mangrove ecosystem. This approach challenges for elevating pollen floras at the same step of botanical relevance than macrofloras, at least at the genus level. In this context, the genus appears to be the most relevant taxonomic entity because (1) most of genera existed from the earliest Paleogene, and (2) its bioclimatic significance is generally well delimited (Harris et al., 2017). The limited identification at the genus level replaces the so-called species, we believe imagined, in most of the previous Paleogene studies.

***Avicennia* (Acanthaceae)**

Because the Early Eocene and Mid-Miocene recorded pollen grains ascribed to *Avicennia* show some morphological variety, we present hereafter three figures with photographs from pollen grains of six modern species (among the eight accepted species by The Plant List, 2013), four from the Western province (*A. bicolor*, *A. germinans*, *A. schaueriana*, *A. tonduzii*; Figures S2–S3), two from the Eastern province (*A. marina*, *A. officinalis*; Fig. S4). Comparisons can be done with ten photographs of *Avicennia* pollen from PETM (Figure S7), thirty-one photographs of *Avicennia* pollen from EECO (Figures S8–S10), sixteen photographs of *Avicennia* pollen from MMCO (Figure S11).

Avicennia shows prolate to spheroidal tricolpate or tricolporate pollen grains characterised by long and largely opened colpi (with or without costae) that makes the polar area (apocolpium) very small and the pollen close to be syncolp(orate). Tricolporate pollen grains show a slightly elongated endoaperture along the polar axis, which does not pass the edges of colpus at the pollen equator. A homobrochate semitectate reticulum constitutes the exine sculpture with dense muri, larger than luminae, which are characterised by a polygonal and slightly elongated outline. Thickness of muri somewhat increases toward the poles that reduces the size of luminae. Colpi are bordered by a thin margo where reticulum is smaller. The structure of the semi-tectate ectexine shows dense columellae with large head constituting the tectum overlying a thinner endexine. At SEM, general shape and exine sculpture can be observed in finer detail showing, in particular, the smooth surface of the tectum somewhat prominent above the columellae. These characters, whatever the pollen is colpate or colporate, are those of the modern *Avicennia* pollen (also supported by an almost similar size), which unique morphology has been extensively described and documented by many photographs at TLM and SEM (Thanikaimoni, 1987; Mao et al., 2012).

Three modern *Avicennia* species display pollen morphologies (with a colpate or colporate apertural system) very close to the *Avicennia* pollen grains of the Early Eocene Arctic–Atlantic: *A. germinans* (L.) L., *A. marina* (Forssl.) Vierh., and *A. officinalis* L. Two of these species (*A. marina* and *A. officinalis*) have pollen grains very close to those recorded in the Mid-Miocene sediments from the Mediterranean region.

Figure S2. Photographs at TLM and SEM of pollen grains of the modern species *Avicennia bicolor* Standl. (slide n° 10887 from the ISEM collection, plant specimen collected in Panama), *A. africana* P.Beauv. = *A. germinans* (L.)L. (slide 875 of the GeoBioStratData collection, plant specimen 14273 from the Herbarium of the University C. Bernard Lyon, France, plant specimen collected in Africa), and *A. tomentosa* Jacq. = *A. germinans* (L.)L. (slide 874 of the GeoBioStratData collection, plant specimen 5 from the Herbarium of the University C. Bernard Lyon, France, plant specimen collected in India) (shots by J.-P. Suc & S.-M. Popescu).
Scale bar = 5 µm.

A. *Avicennia bicolor*.

A1–A4, LO-analysis of equatorial view (aperture facing): A1, reticulate ornamentation; A2, focus at base of columellae; A3, ecto- and endo-apertures; A4, optical section.

A5–A8, LO-analysis of polar view: A5, reticulate ornamentation; A6, focus at base of columellae; A7, apocolpium; A8, optical section.

B, *Avicennia africana* = *A. germinans*.

B1–B4, LO-analysis of equatorial view (intercolpium): B1, reticulate ornamentation; B2, focus at base of columellae; B3, colpi; B4, optical section.

B5–B6, LO-analysis of polar view: B5, reticulate ornamentation; B6, optical section.

B7, Equatorial overview (aperture facing).

B8, Polar overview.

C, *Avicennia tomentosa* = *A. germinans*.

C1–C4, LO-analysis of equatorial view (aperture facing): C1, reticulate ornamentation; C2, focus at base of heads of columellae, ectoaperture; C3, focus at base of columellae; C4, optical section.

C5–C6, LO-analysis of polar view: C5, reticulate ornamentation and focus at base of columellae; C6, optical section.

C7, equatorial overview (intercolpium).

C8, polar overview.

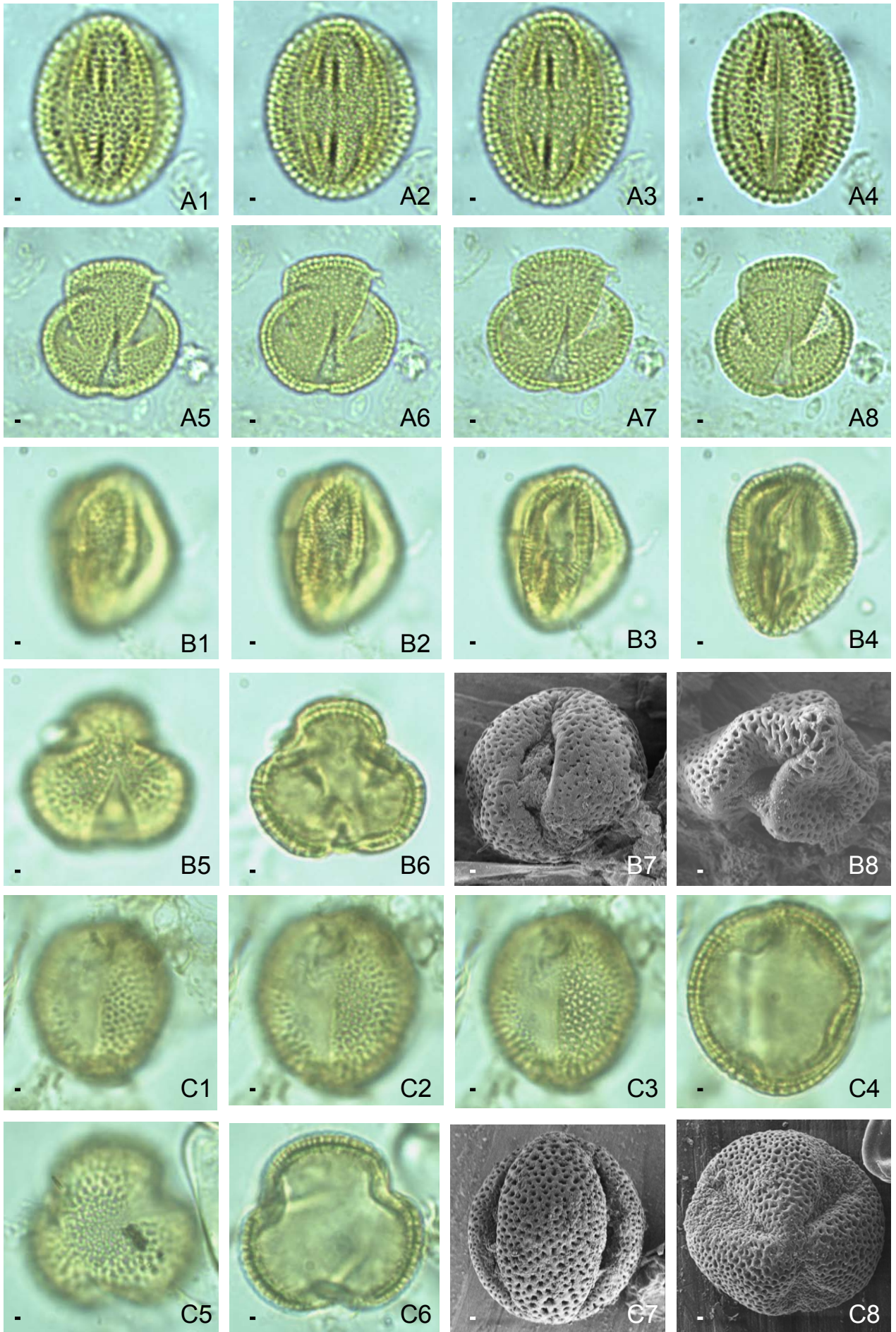


Figure S3. Photographs at TLM of pollen grains of the modern species *Avicennia schaueriana* Stapf & Leechm. ex Moldenke (slide 10886 from the ISEM collection, plant specimen collected in the West Indies) and *A. tonduzii* Moldenke (slide 10885 from the ISEM collection, plant specimen collected at Costa Rica) (shots by J.-P. Suc & S.-M. Popescu). Scale bar = 5 μ m.

A. *Avicennia schaueriana*.

A1–A3, LO-analysis of equatorial view (aperture facing): A1, reticulate ornamentation; A2, focus at base of columellae; A3, optical section.

A4–A6, LO-analysis of polar view: A4, reticulate ornamentation; A5, focus at base of columellae; A6, optical section.

B. *Avicennia tonduzii*.

B1–B3, LO-analysis of equatorial view (aperture facing): B1, reticulate ornamentation; B2, focus at base of columellae; B3, optical section.

B4–B6, LO-analysis of polar view: B4, reticulate ornamentation; B5, focus at base of columellae; B6, optical section.

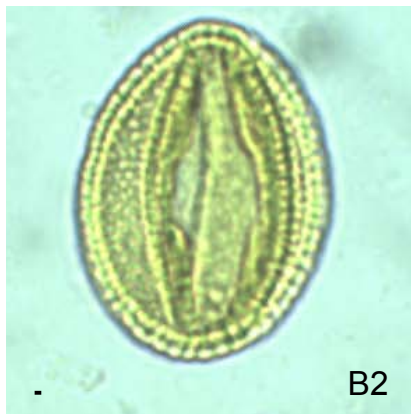
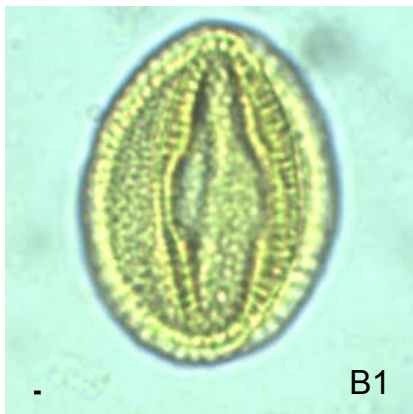
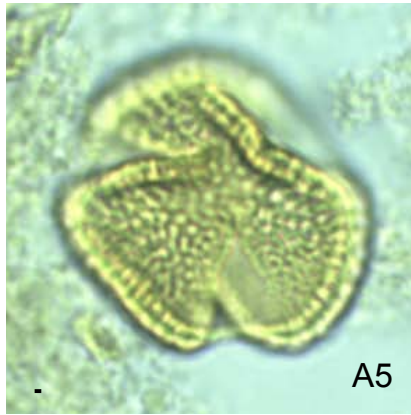


Figure S4. Photographs at TLM and SEM of pollen grains of the modern species *Avicennia alba* Blume = *A. marina* (Forssk.) Vierh. and *A. officinalis* L. (shots by J.-P. Suc & S.-M. Popescu).

Scale bar = 5 μm .

A, *Avicennia alba* = *A. marina*.

A1–A4, LO-analysis of equatorial view (intercolpium): A1, reticulate ornamentation; A2, focus at base of columellae; A3, colpi; A4, optical section.

A5–A6, LO-analysis of polar view: A5, reticulate ornamentation and focus at base of columellae; A6, optical section.

A7, Equatorial overview (aperture facing).

A8, Polar overview.

B, *Avicennia officinalis*.

B1–B4, LO-analysis of equatorial view (intercolpium): B1, reticulate ornamentation; B2, focus at base of columellae; B3, colpi; B4, optical section.

B5–B7, LO-analysis of equatorial view (aperture facing): B5, reticulate ornamentation; B6, focus at base of columellae; B7, optical section.

B8–B11, LO-analysis of polar view: B8, reticulate ornamentation; B9, focus at base of columellae; B10, apocolpium; B11, optical section.

B12, Equatorial overview (intercolpium).

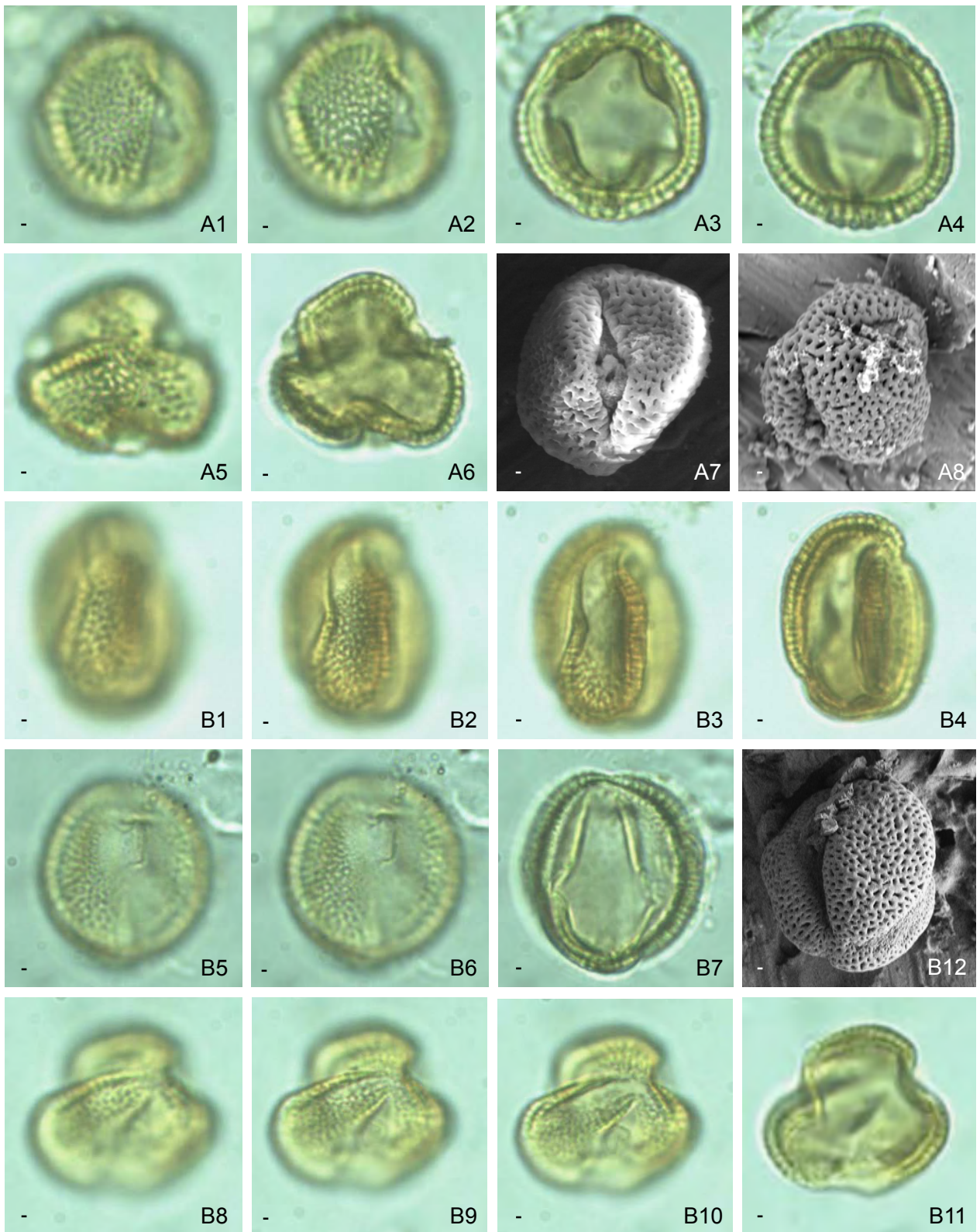


Figure S5. Photographs at TLM of pollen grains of the modern species *Pelliciera rhizophorae* Planch. & Triana (Tetrameristaceae) (slide 38826 from the ISEM collection) and Rhizophoraceae: *Rhizophora candelaria* DC. = *R. apiculata* Blume (slide 34256 from the ISEM collection, plant specimen collected in India), *R. mucronata* Lam. (slide 10833 from the ISEM collection), *Bruguiera parviflora* (Roxb.) Wright & Arn. ex Griff. (slide 40409 from the ISEM collection), *Ceriops roxburghiana* Arn. = *C. decandra* (Griff.) W.Theob. (slide 15072 from the ISEM collection, plant specimen collected in India) (shots by J.-P. Suc & S.-M. Popescu). Scale bar = 5 µm.

A, *Pelliciera rhizophorae*.

A1, Equatorial view (aperture facing), optical section.

A2, Polar view, optical section.

B, *Rhizophora candelaria* = *R. apiculata*.

B1–B2, LO-analysis of equatorial view (aperture facing): B1, microreticulate ornamentation; B2, optical section.

B3–B4, LO-analysis of equatorial view (intercolpium): B3, microreticulate ornamentation; B4, optical section.

B5–B6, LO-analysis of polar view: B5, microreticulate ornamentation; B6, optical section.

C, *Rhizophora mucronata*.

C1–C2, LO-analysis of equatorial view (aperture facing): C1, scabrate ornamentation; C2, optical section.

C3–C4, LO-analysis of polar view: C3, scabrate ornamentation; C4, optical section.

D, *Bruguiera parviflora*.

D1–D2, LO-analysis of equatorial view (aperture facing): D1, scabrate ornamentation; D2, optical section.

D3–D4, LO-analysis of polar view: D3, scabrate ornamentation; D4, optical section.

E, *Ceriops roxburghiana* = *C. decandra*.

E1–E2, LO-analysis of equatorial view (aperture facing): E1, scabrate ornamentation; E2, optical section.

E3, Polar view, optical section.

***Pelliciera rhizophorae* Planch. & Triana (Tetrameristaceae) (Figure S5, A1–A2).**

The great-sized spheroidal pollen of this species is tricolporate with thin and relatively short colpi as ectoapertures that confers a large apocolpial field in polar view. The endoapertures are perpendicular to the ectoapertures delimited by slightly marked costae discontinuous at the equator. The pollen is tectate with relatively thick endexine and ectexine, which shows a foveolate-fossulate to verrucate-rugulate ornamentation. This pollen morphology is described and illustrated by Thanikaimoni (1887).

Rhizophoraceae (Figure S5, B1–E2).

The mangrove genera of Rhizophoraceae show an almost similar pollen morphology. Slightly prolate to spheroidal, the pollen is tricolporate, sometimes tetracolporate, with long ectoapertures and perpendicular long endoapertures bordered by prominent costae. Rounded triangular polar view shows vestibula. Ectexine, thicker than endexine, shows a variable ornamentation, scabrate to microreticulate or foveolate. In addition to variability in pollen size, such a homogenous morphology makes very difficult the identification of genera according to pollen.

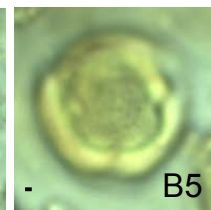
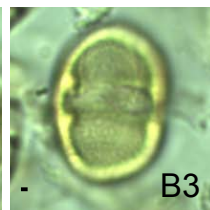


Figure S6. Photographs at TLM of pollen grains of the modern species *Nypa fruticans* Wurm (Arecaceae) (slide 34258 from the ISEM collection, plant specimen collected in India), *Tarrietia perakensis* King = *Heritiera sumatrana* (Miq.) Kosterm. (Malvaceae) (slide 17929 from the ISEM collection, plant specimen collected in Malaysia), *Scyphiphora hydrophylacea* C.F.Gaertn. (Rubiaceae) (slide 21266 from the ISEM collection, plant specimen collected at Singapore), *Brownlowia argentata* Kurz (Malvaceae) (slide 20764 from the ISEM collection, plant specimen collected in Indonesia), *Brownlowia elata* Roxb. (Malvaceae) (slide 19839 from the ISEM collection, plant specimen collected in Burma), *Xylocarpus mekongensis* Pierre (Meliaceae) (slide 11310 from the ISEM collection, plant specimen collected in India), *Sonneratia caseolaris* (L.)Engl. (Lythraceae) (slide 653 of the GeoBioStratData collection), *Excoecaria agallocha* L. (Euphorbiaceae) (slide 11306 from the ISEM collection, plant specimen collected in Vietnam) (shots by J.-P. Suc & S.-M. Popescu). Scale bar = 5 μ m.

A, *Nypa fruticans*.

A1, Equatorial view (aperture facing), optical section.

B, *Tarrietia perakensis* = *Heritiera sumatrana*.

B1–B2, LO-analysis of equatorial view (aperture facing): B1, reticulate ornamentation; B2, optical section.

C, *Scyphiphora hydrophylacea*.

C1–C2, LO-analysis of equatorial view (aperture facing): C1, reticulate ornamentation; C2, focus at base of columellae and colporus.

C3–C4, LO-analysis of polar view: C3, reticulate ornamentation; C4, optical section.

D, *Brownlowia*.

D1–D2, *Brownlowia argentata*, LO-analysis of polar view: D1, reticulate ornamentation; D2, optical section.

D3–D4, *Brownlowia elata*, LO-analysis of polar view: D3, reticulate ornamentation; D4, optical section.

E, *Xylocarpus mekongensis*.

E1, Polar view of a tetracolporate pollen, optical section.

E2, Polar view of a tricolporate pollen, optical section.

F, *Sonneratia caseolaris*.

F1–F2, LO-analysis of equatorial view (aperture facing): F1, verrucate ornamentation; F2, optical section.

G, *Excoecaria agallocha*.

G1–G4, LO-analysis of equatorial view (aperture facing): G1, finely reticulate ornamentation; G2, focus at base of columellae; G3, colporus; G4, optical section.

G5, polar view, optical section.

Nypa fruticans Wurm (Arecaceae) (Figure S6, A1).

Large spheroidal to elliptical pollen, monocolpate, with long spines, finely reticulate in between spines.

Tarrietia perakensis King = *Heritiera sumatrana* (Miq.) Kosterm. (Malvaceae) (Figure S6, B1–B2).

Small prolate spheroidal pollen, tricolporate, finely reticulate. Ectoapertures (colpi) are long with thin costae, endoapertures (pori) are small and weakly annulate.

Scyphiphora hydrophylacea C.F.Gaertn. (Rubiaceae) (Figure S6, C1–C4).

Large spheroidal pollen, tricolporate, with reticulate ornamentation. Endoapertures (pori) are bordered by a thick annulus.

Brownlowia argentata Kurz and *Brownlowia elata* Roxb. (Malvaceae) (Figure S6, D1–D4).

Oblate pollen, tricolporate, interaperturate with marked costae along the short ectoapertures, reticulate ornamentation of the thick ectexine.

Xylocarpus mekongensis Pierre (Meliaceae) (Figure S6, E1–E2).

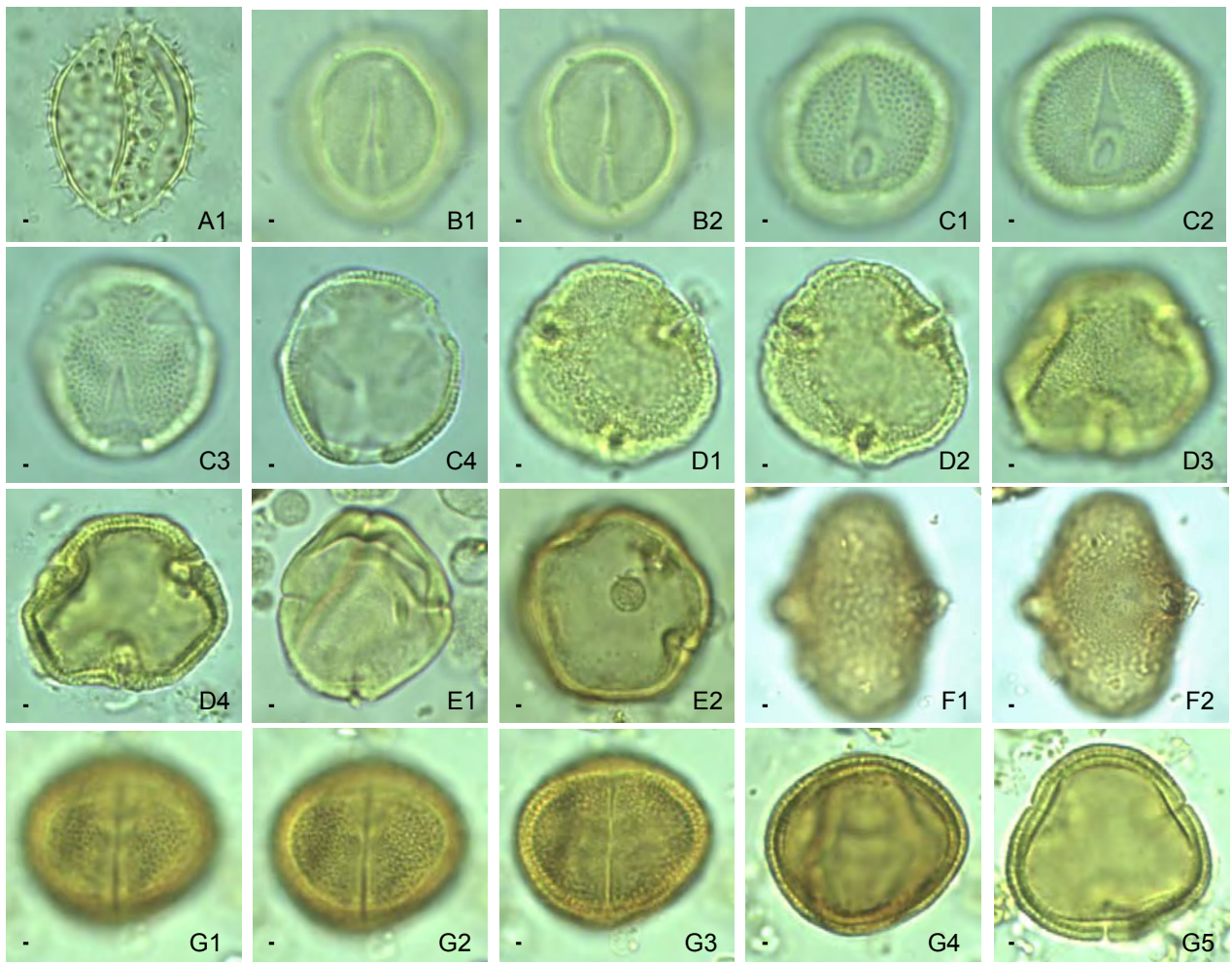
Oblate pollen, tricolporate to tetracolporate, scabrate. Ectoapertures (colpi) are very short, endoapertures (pori) are bordered by a thick discontinuous annulus.

Sonneratia caseolaris (L.)Engl. (Lythraceae) (Figure S6, F1–F2).

Large prolate pollen, triporate, granulate to verrucate ornamentation. Apertures (pori) are circular, prominently protruding and bordered by a thin annulus.

Excoecaria agallocha L. (Euphorbiaceae) (Figure S6, G1–G5).

Prolate to oblate pollen, tricolporate, finely reticulate ornamentation. Ectoapertures are long, endoapertures narrowly elliptic.



Fossil pollen flora

Figures S6–S10 display photographs of fossil pollen grains ascribed to mangrove taxa from PETM, EECO and MMCO samples.

To complete our iconography of *Avicennia* fossil pollen grains, it is to be specified that the pollen grains published as *Gunnera* by Palacios Chavez & Rzedowski (1993: Plate XXIV, Fig. 479) and as *Retitricolpites* sp. by Médus (1975: Plate XIV, Figs. 27–28) probably belong to *Avicennia*.

Comment about the *Sonneratia*-type pollen. Only seven pollen grains (from Gan, Kallo, Morlaàs 1, Site 547 and Site 918) have been recorded showing a morphology evoking that of *Sonneratia*. The best preserved pollen of this group is shown in Figure S9 (C1–C2). These pollen grains, similar to that published by Gruas-Cavagnetto et al. (1988) from Thanetian of Southern France, are characterised by mesocolpal ridges, a verrucate equatorial belt, and no distinctive polar caps: according to Mao and Foong (2013), they are possibly assignable to the fossil genus *Florschuetzia*, a potential precursor of the extant *Sonneratia* genus. Waiting for more records of such pollen grains, we chose to group them within the term *Sonneratia*-type.

Figure S7. Photographs at TLM of fossil pollen grains from PETM sediments – location number refer to Figure 2 (shots by J.-P. Suc & S.-M. Popescu).

Scale bar = 5 μm .

A, *Avicennia*.

A1–A2, Site M0004A (location 1), 382.44 mbsf: A1, cluster of pollen grains; A2, polar view.

A3, Faddeevsky Island (location 2), sample GS127, polar view.

A4–A6, Site 918 (location 5), 1180.49 mbsf: A4–A5, equatorial view (aperture facing); A6, polar view.

A7, Site 918 (location 5), 1180.71 m, equatorial view (aperture facing).

A8–A10, Site 547 (location 11), equatorial views (aperture facing): A8, 279.31 mbsf; A9–A10, 279.53 mbsf.

B, *Brownlowia*.

B1–B2, Site 918 (location 5), 1180.49 mbsf, LO-analysis polar view: B1, reticulate ornamentation; B2, optical section.

C, Rhizophoraceae.

C1, Site 918 (location 5), 1180.49 mbsf, equatorial view (aperture facing).

C2, Site 547 (location 11), 279.31 mbsf, equatorial view (aperture facing).

C3–C4, Site 547 (location 11), 279.53 mbsf, equatorial view (aperture facing).

D, *Xylocarpus*.

D1, Noirmoutier (location 7), sample 2, equatorial view (intercolpium).

D2, Site 547 (location 11), 279.31 mbsf, polar view.

E, *Nypa*.

E1, Noirmoutier (location 7), sample 2, optical section.

E2, Calavanté 1 (location 8), 3402 m, optical section.

F, *Excoecaria*.

F1–F2, Site 547 (location 11), 279.53 mbsf, LO-analysis of equatorial view (intercolpium):

F1, reticulate ornamentation; F2, optical section.

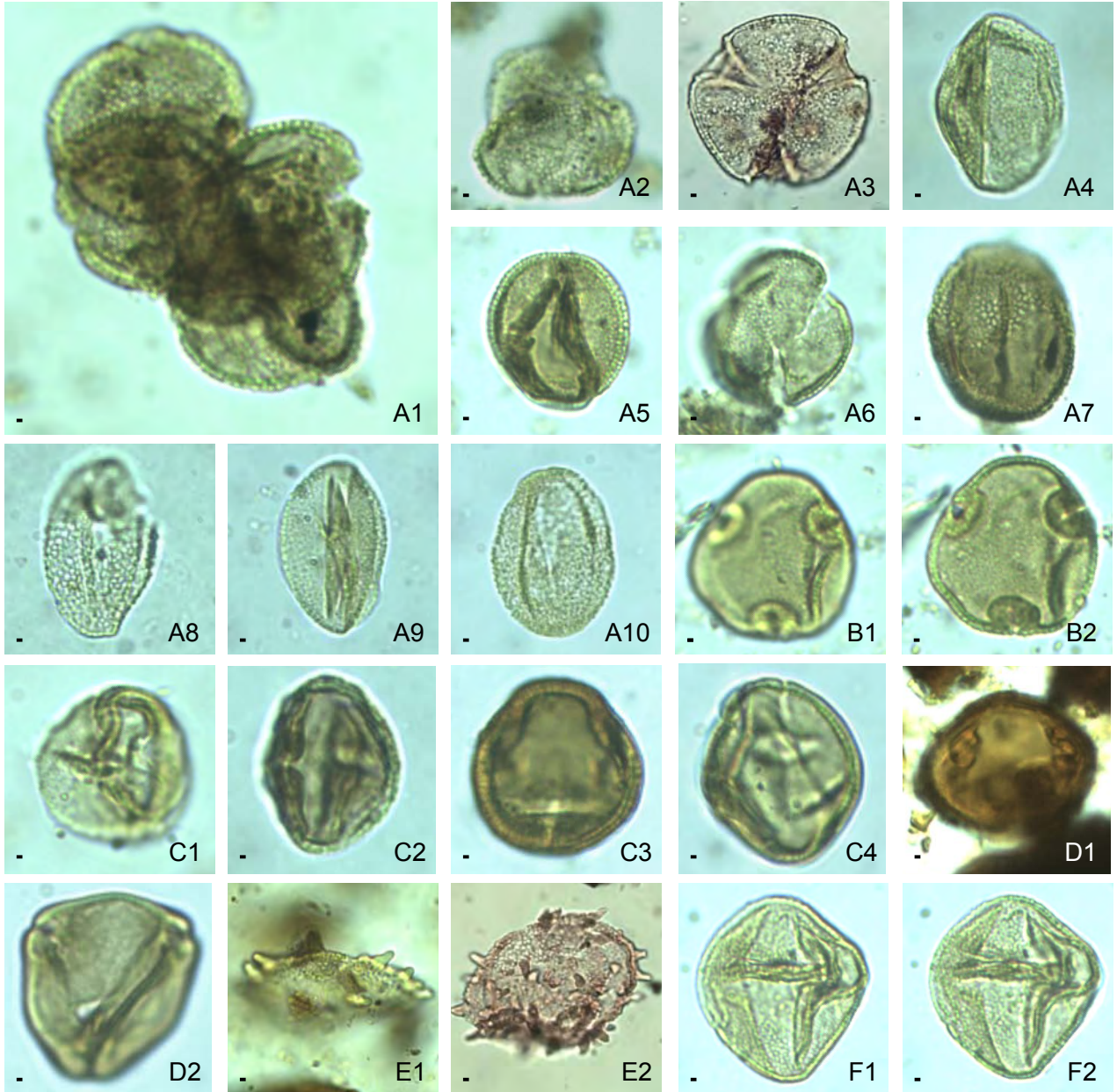


Figure S8. Photographs at TLM and SEM of fossil pollen grains from EECO sediments – location numbers refer to Figure 2 (shots by J.-P. Suc & S.-M. Popescu). Scale bar = 5 μm .

A, *Avicennia*.

A1–A2, Site M0004A (location 1), 318.86 mbsf, LO-analysis of equatorial view (aperture facing): A1, reticulate ornamentation; A2, aperture.

A3, Site M0004A (location 1), 313.41 mbsf, equatorial view (aperture facing).

A4–A5, Site M0004A (location 1), 297.72 mbsf, equatorial view: A4, intercolpium; A5, aperture facing.

A6, M0004A (location 1, 301.53 mbsf, equatorial view (intercolpium).

A7, M0004A (location 1), 318.86 mbsf, equatorial view (intercolpium).

A8–A9, M0004A (location 1), 287.395 mbsf, equatorial view (intercolpium), reticulate ornamentation.

A10–A12, Caribou Hills (location 3), sample 18, polar view: A10, optical section; A11, reticulate ornamentation; A12, reticulate ornamentation.

A13, Caribou Hills (location 3), sample 12, polar view, reticulate ornamentation.

A14, Caribou Hills (location 3), sample 18, equatorial view (aperture facing), optical section.

A15–A16, Caribou Hills (location 3), sample 18, equatorial overview (intercolpium).

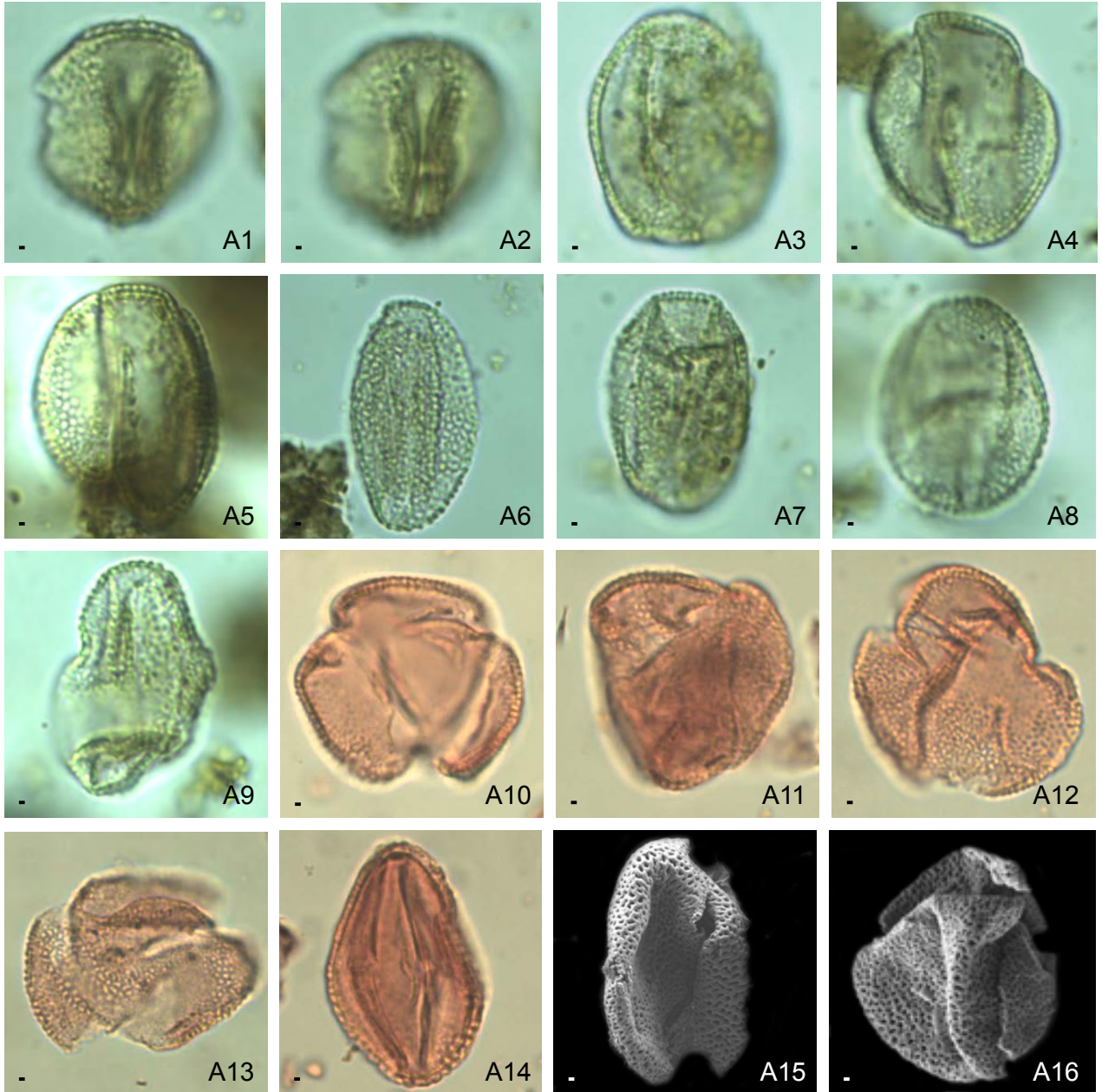


Figure S9. Photographs at TLM of fossil pollen grains from EECO sediments – location numbers refer to Figure 2 (shots by J.-P. Suc & S.-M. Popescu).
Scale bar = 5 μ m.

A, *Avicennia*.

A1–A6, Site 343 (location 4).

A1–A3, 213.995 mbsf, equatorial view: A1, intercolpium, reticulate ornamentation; A2–A3, aperture facing, reticulate ornamentation.

A4–A6, 214.30 mbsf, equatorial view (intercolpium): A4–A5, reticulate ornamentation; A6, optical section.

A7–A12, Site 918 (location 5).

A7, 1157.21 mbsf: polar view, reticulate ornamentation.

A8–A9, 1156.71 mbsf, LO-analysis of polar view: A8, reticulate ornamentation; A9, optical section.

A10, 1157.71 mbsf: polar view, optical section.

A11–A12, 1158.21 mbsf: A11, polar view, optical section; A12, equatorial view (aperture facing), reticulate ornamentation.

B, *Excoecaria*.

B1–B3, Site 343 (location 4), 213.995 mbsf, LO-analysis of equatorial view (intercolpium):

B1, microreticulate ornamentation; B2, optical section; B3, aperture.

C, Rhizophoraceae.

C1–C2, Site 343 (location 4), 214.3 mbsf, equatorial view (aperture facing): C1, ornamentation; C2, aperture.

C3–C5, Site 343 (location 4), 213.995 mbsf, LO-analysis of equatorial view (aperture facing): C3, ornamentation, aperture; C4, aperture; C5, optical section.

C6–C7, Site 918, 1158.21 mbsf, LO-analysis of equatorial view (aperture facing): C6, ornamentation and aperture; C7, optical section.

D, *Xylocarpus*.

D1–D3, Site 343 (location 4), 214.3 mbsf, LO-analysis of polar view: D1, finely reticulate ornamentation; D2, aperture; D3, optical section.

E, *Scyphiphora*.

E1–E2, Site 343 (location 4), 213.995 mbsf, LO-analysis of polar view: E1, ornamentation and apertures; E2, optical section.

F, *Brownlowia*.

F1–F2, Site 918 (location 5), 1158.21 mbsf, polar view: F1, ornamentation; F2, optical section.

G, *Heritiera*.

G1, Site 918 (location 5), 1158.21 mbsf, polar view.

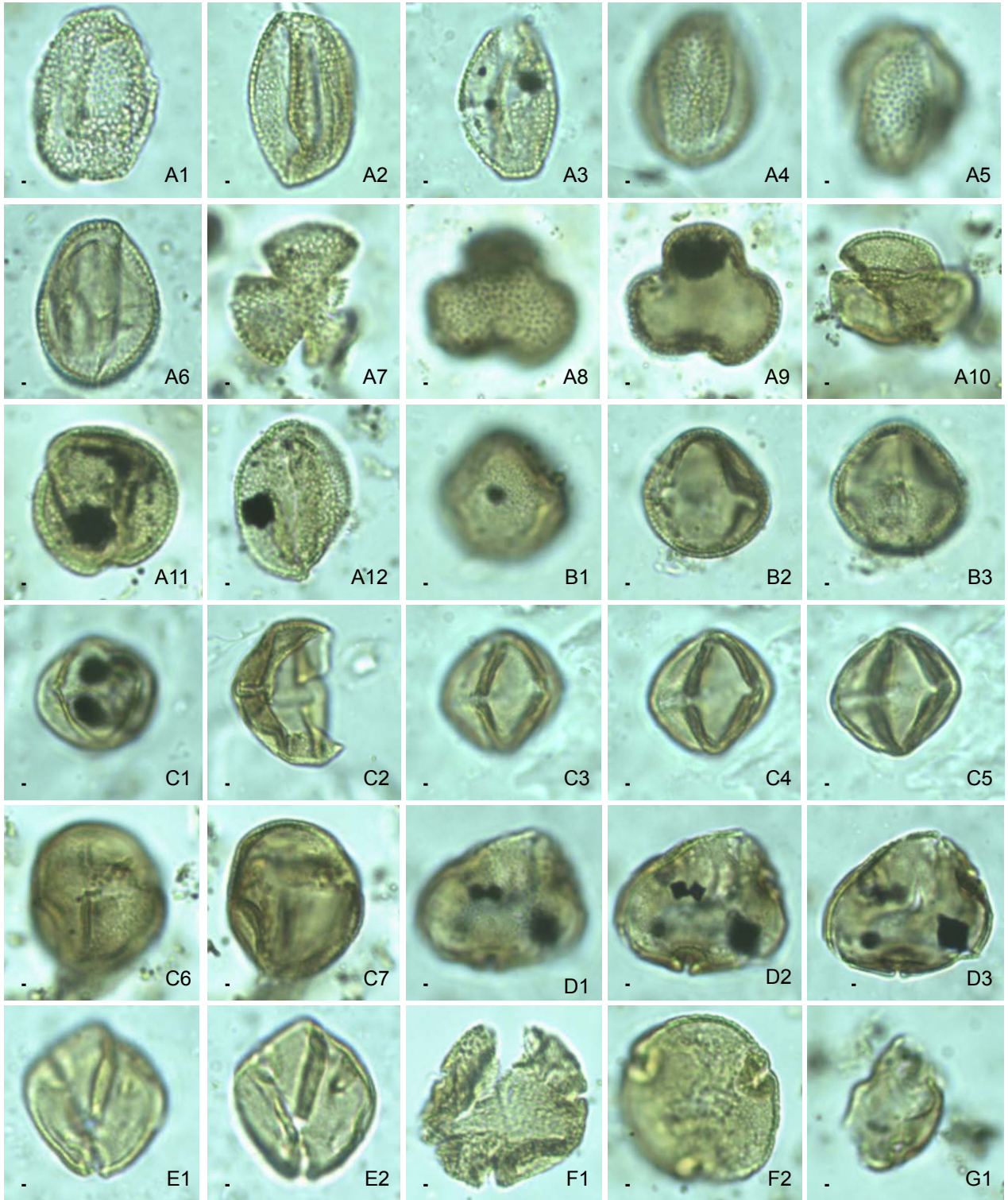


Figure S10. Photographs at TLM and SEM of fossil pollen grains from EECO sediments – location numbers refer to Figure 2 (shots by J.-P. Suc & S.-M. Popescu).
Scale bar = 5 µm.

A, *Avicennia*.

A1–A3, Kallo 027E148 (location 6).

A1–A2, 239 m, LO-analysis of equatorial view (aperture facing): A1, reticulate ornamentation; A2, optical section.

A3, 265 m, equatorial view (intercolpium), reticulate ornamentation.

A4, Morlaàs 1 (location 9), 1282 m, equatorial view (intercolpium), reticulate ornamentation.

B, *Nypa*.

B1, Kallo 027E148 (location 6), 286.5 m, reticulate ornamentation and optical section.

B2–B3, Gan (location 10), sample 1: B2, overview; B3, optical section.

C, *Sonneratia*-type.

C1–C2, Kallo 027E148 (location 6) 286.5 m, LO-analysis of equatorial view (intercolpium):

C1, verrucate ornamentation; C2, aperture and optical section.

D, *Xylocarpus*.

D1, Morlaàs 1 (location 9), 1462 m, polar view, optical section.

E, *Pelliciera*.

E1, Morlaàs 1 (location 9), 1462 m, polar view, apertures and optical section.

F, Rhizophoraceae.

F1, Morlaàs 1 (location 9), 1462 m, equatorial view (aperture facing), ornamentation.

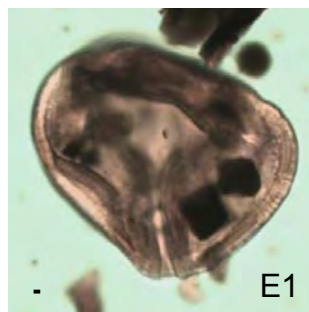
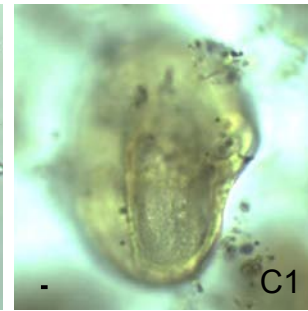
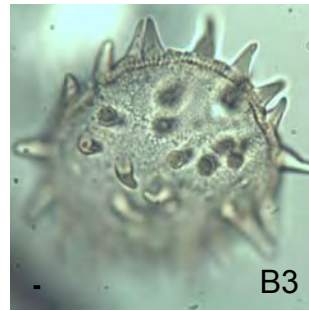
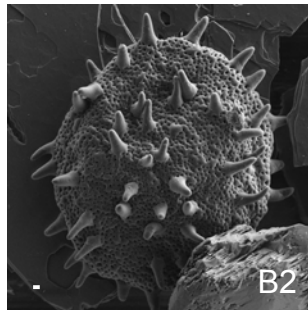
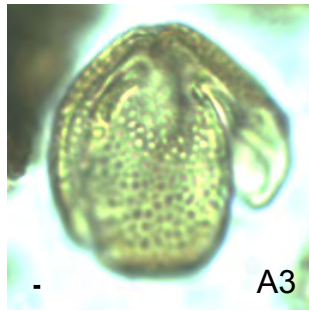
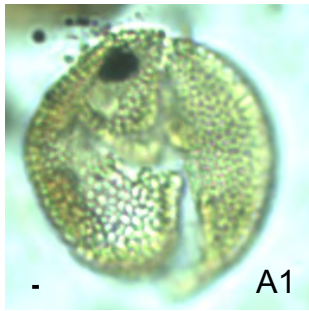


Figure S11. Photographs at TLM and SEM of fossil pollen grains from MMCO sediments – location numbers refer to Figure 3 (shots by J.-P. Suc & S.-M. Popescu). Scale bar = 5 μm .

A, Avicennia.

A1–A2, La Rierussa (location 7), sample 1, equatorial view (aperture facing): A1, reticulate ornamentation; A2, optical section.

A3, Saint-Geniès (location 6), equatorial view (intercolpium), overview.

A4–A13, Estagel (location 5), sample 8.

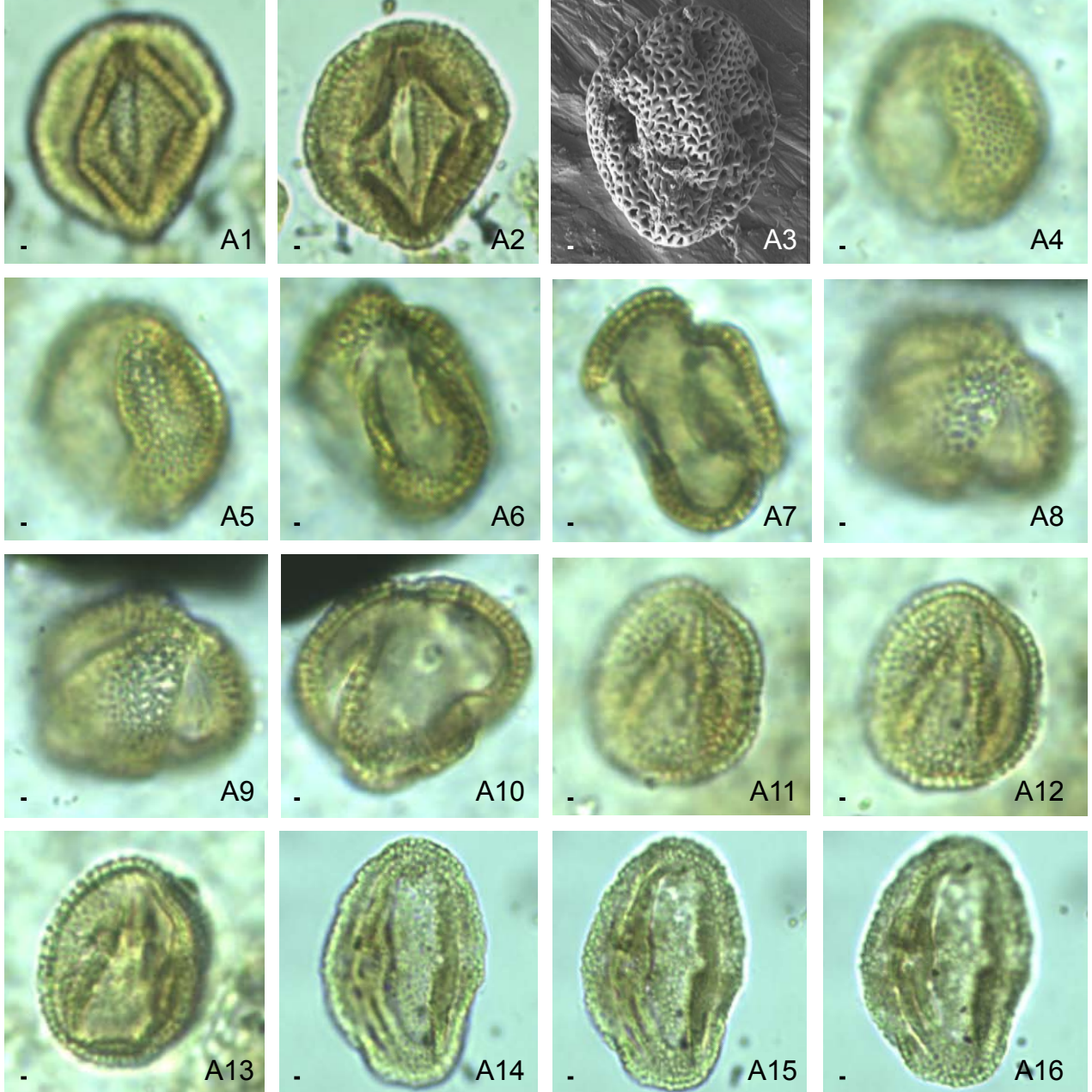
A4–A5, equatorial view (intercolpium): A4, reticulate ornamentation; A5, focus at base of columellae and optical section.

A6–A7, polar view: A6, reticulate ornamentation; A7, optical section.

A8–A10, polar view: A8, reticulate ornamentation; A9, focus at base of columellae; A10, optical section.

A11–A13, equatorial view (aperture facing): A11, reticulate ornamentation; A12, focus at base of columellae; A13, optical section.

A14–A16, Göllersdorf (location 1), sample 22, equatorial view (intercolpium): A14, reticulate ornamentation; A15, optical section; A16, apertures.



References

- Erdtman, G. (1952). *Pollen morphology and plant taxonomy*. Angiosperms. Almqvist and Wiksell, Stockholm.
- Gruas-Cavagnetto, C., Tambareau, Y., & Villatte, J. (1988). Données paléoécologiques nouvelles sur le Thanétien et l'Ilerdien de l'avant-pays pyrénéen et de la Montagne Noire. *Institut français de Pondichéry, Travaux de la Section Scientifique et Technique*, 25, 219–235.
- Harris, A., Dee, J., & Palmer, M.W. (2017). The effects of taxonomic rank on climatic calibrations: a test using extant floras of United States counties. *Review of Palaeobotany and Palynology*, 244, 316–324.
- Mao, L., Batten, D.J., Fujiki, T., Li, Z., Dai, L., & Weng, C. (2012). Key to mangrove pollen and spores of southern China: an aid to palynological interpretation of Quaternary deposits in the South China Sea. *Review of Palaeobotany Palynology*, 176–177, 41–67.
- Mao, L., & Foong, S.Y. (2013). Tracing ancestral biogeography of *Sonneratia* based on fossil pollen and their probable modern analogues. *Palaeoworld*, 22, 133–143.
- Médus, J. (1975). Palynologie de sediments tertiaries du Sénégal méridional. *Pollen et Spores*, 17(4), 545–608.
- Nix, H. (1982). Environmental determinants of biogeography and evolution in Terra Australis, in: Barker, W.R., Greenslade, P.J.M. (Eds.), *Evolution of the Flora and fauna of Arid Australia*. Peacock Publishing, Frewville, pp. 47–66.
- Palacios Chavez, R., & Rzedowski, J. (1993). Estudio palinologico de las floras fosiles del Miocene inferior y principios del Miocene medio de la region de Pichucalco, Chiapas, Mexico. *Acta Botánica Mexicana*, 24, 1–96.
- Punt, W., Hoen, P.P., Blackmore, S., Nilsson, S., & Le Thomas, A. (2007). Glossary of pollen and spore terminology. *Review of Palaeobotany and Palynology*, 143, 1–81.
- Thanikaimoni, G. (1987). Mangrove Palynology. Institut Français de Pondichéry. *Travaux de la Section Scientifique et Technique*, 24, 1–100.
- The Plant List (2013). Version 1.1. Published on the Internet <http://www.theplantlist.org/>.